

MULTI-MESSENGER INSIGHTS INTO ULTRA-HIGH-ENERGY COSMIC RAYS FROM FRO RADIO GALAXIES: EMISSION SPECTRUM, COMPOSITION, AND SECONDARY PHOTONS AND NEUTRINOS

Jon Paul Lundquist
jplundquist@gmail.com



University of
Nova Gorica

www.ung.si/en/research/cac/



7th International Symposium on Ultra High Energy Cosmic Rays
(UHECR) 2024

17-21 Nov 2024, Malargüe, Mendoza, Argentina

**“Combined Fit of Spectrum and Composition for FR0 Radio Galaxy Emitted
Ultra-High-Energy Cosmic Rays with Resulting Secondary Photons and Neutrinos”**

arXiv:2407.06961 Accepted for Publication in ApJ

**Jon Paul Lundquist¹, Serguei Vorobiov¹, Lukas Merten², Anita Reimer², Margot
Boughelilba², Paolo Da Vela², Fabrizio Tavecchio³, Giacomo Bonnoli³, Chiara Righi³**

¹*Center for Astrophysics and Cosmology (CAC), University of Nova Gorica, Nova Gorica, Slovenia*

²*Institute for Astro and Particle Physics, University of Innsbruck, Innsbruck, Austria*

³*Astronomical Observatory of Brera, Milano, Italy*



University of
Nova Gorica



ABSTRACT SUMMARY



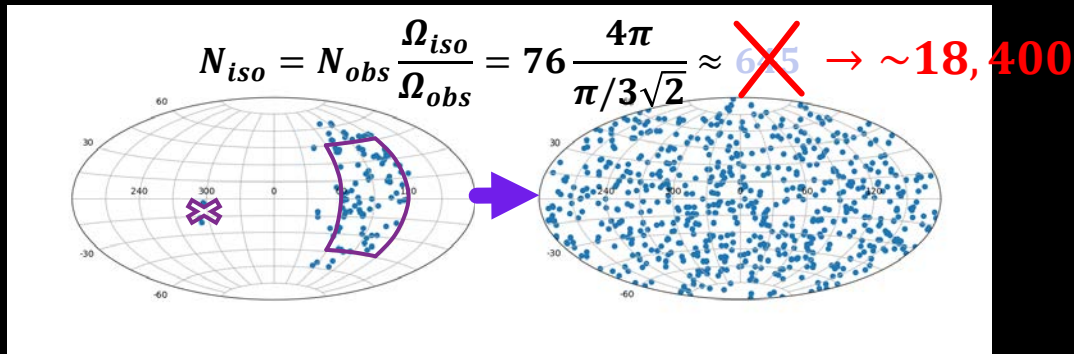
- Low luminosity Fanaroff-Riley Type 0 (FR0) radio galaxies can be significant UHECR flux contributors[1].
 - FR0 outnumber more powerful FR radio galaxies by $\sim 5x$ ($z < 0.05$).
- Presented is a comprehensive CRPropa3 simulation study to estimate mass composition and energy spectra of UHECRs emitted by FR0.
 - Integrates FR0 properties[2] and intergalactic magnetic fields (random and structured).
- Fitting spectral indices, rigidity cutoffs, and elemental fractions to Pierre Auger Observatory's spectrum and composition, probes the FR0 source contribution.
- Secondary photon and neutrino fluxes from cosmic photon background interactions are compared with current upper limits and theoretical models.
- This multi-messenger approach provides insights into the role of FR0 within the UHECR landscape.

Cheng et al. 2021, MNRAS

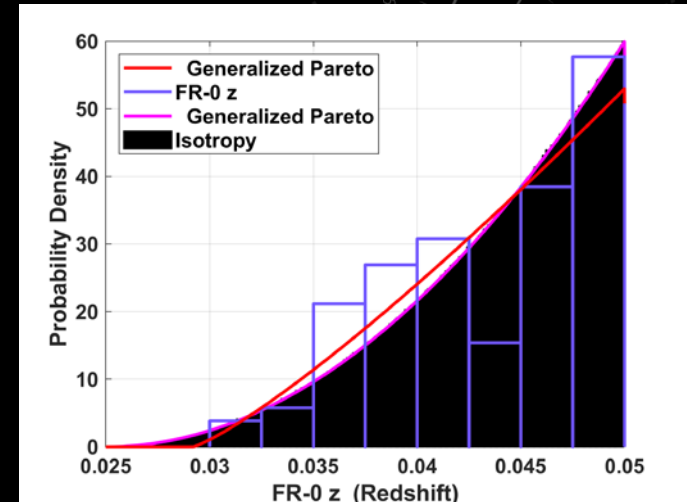
[1] Merten, L. et al., Scrutinizing FR 0 radio galaxies as ultra-high-energy cosmic ray source candidates, *Astropart. Phys.* 128 (2021) 102564.

[2] Baldi, R. D. et al., FROCAT: a FIRST catalog of FR 0 radio galaxies, *A&A* 609 (2018) A1.

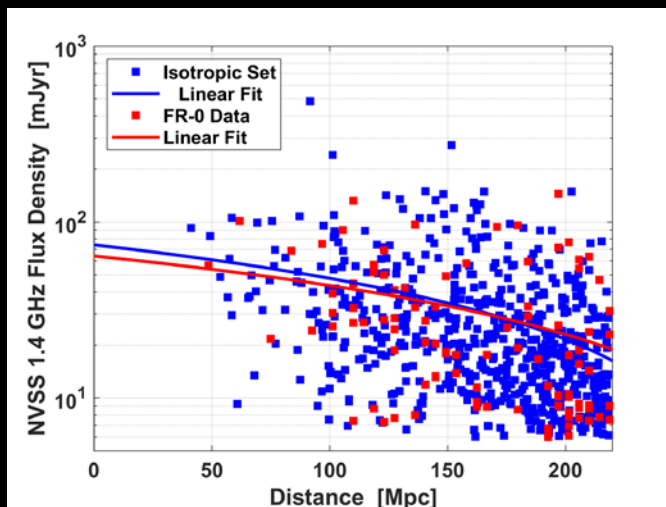
ISOTROPIC FR-0 SIMULATION



Full-sky isotropic FR0 radio galaxy density estimated from well-sampled FROCAT[1] catalog section.

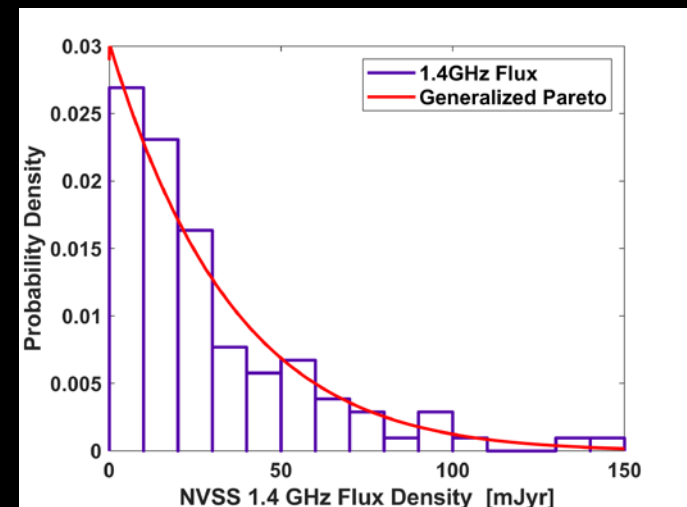


Simulated FR0 redshift distribution from Pareto fit to catalog data[1]. Isotropy p-val = ~16%.



Previous results:
 $z \leq 0.05$
 Update:
 $z \leq 0.2$

Source evolution modeled by preserving radio output and redshift-distance correlation (Kendall Corr. Coeff: -0.28, p-val: 4.6e-5)[1].



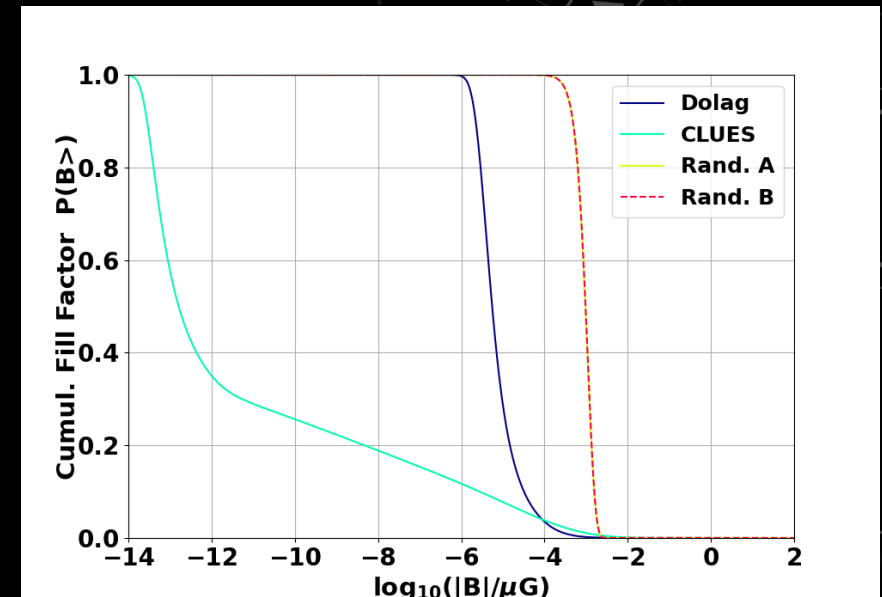
FR0 UHECR flux proportional to radio output. Generated by Pareto fit to NVSS data[1].

CONSTANT FRACTION FIT

The background features several faint, stylized circular gauges and arrows. One large gauge in the upper right quadrant has a scale from 80 to 210. Another gauge in the lower right quadrant has a scale from 0 to 100. A third gauge in the lower left quadrant has a scale from 0 to 100. Arrows of various sizes and orientations are scattered throughout the background, some pointing clockwise and others counter-clockwise.

MODELS AND COMBINED FIT – CONSTANT FRACTION

- **Three EAS Models:** SIBYLL2.3c, EPOS-LHC and **QGSJETII-04**
- **Two Structured Fields:** *Tables in appendix*
 - Dolag et al. [arXiv:0410419](https://arxiv.org/abs/0410419)
 - CLUES -- Hackenstein et al. (Astro_1B): [arXiv:1710.01353](https://arxiv.org/abs/1710.01353)
- **Two 1 nG Random Fields:**
 - A: $\langle l_{\text{corr}} \rangle = 234$ kpc, B: $\langle l_{\text{corr}} \rangle = 647$ kpc
- **And no magnetic Field**



Minimize

$$\sum \chi_{\text{tot}}^2 / \text{dof} = \sum \chi_E^2 / \text{dof}_E + \sum \chi_C^2 / \text{dof}_C$$

- **8 Parameters:**
 - Power law: γ
 - Spectrum normalization: n
 - Exponential cut off: ZR_{cut}
 - 5 nuclei: H, He, N, Si, Fe.
 - $\sum f_a = 100\% \rightarrow 4$ parameters.
 - Maximum trajectory D

- CRPropa3 sim. power law $\gamma = 1$
- Reweight simulated events.

$$\frac{dN_A}{dE} = J_A(E) = f_A J_0 \left(\frac{E}{10^{18} \text{ eV}} \right)^{-\gamma} \times f_{\text{cut}}(E, Z_A R_{\text{cut}})$$

$$f_{\text{cut}}(E, Z_A R_{\text{cut}}) = \begin{cases} 1 & (E < Z_A R_{\text{cut}}) \\ \exp\left(1 - \frac{E}{Z_A R_{\text{cut}}}\right) & (E > Z_A R_{\text{cut}}) \end{cases}$$

- Constant nuclei fraction: f_A
- Rigidity dependent cutoff: ZR_{cut}

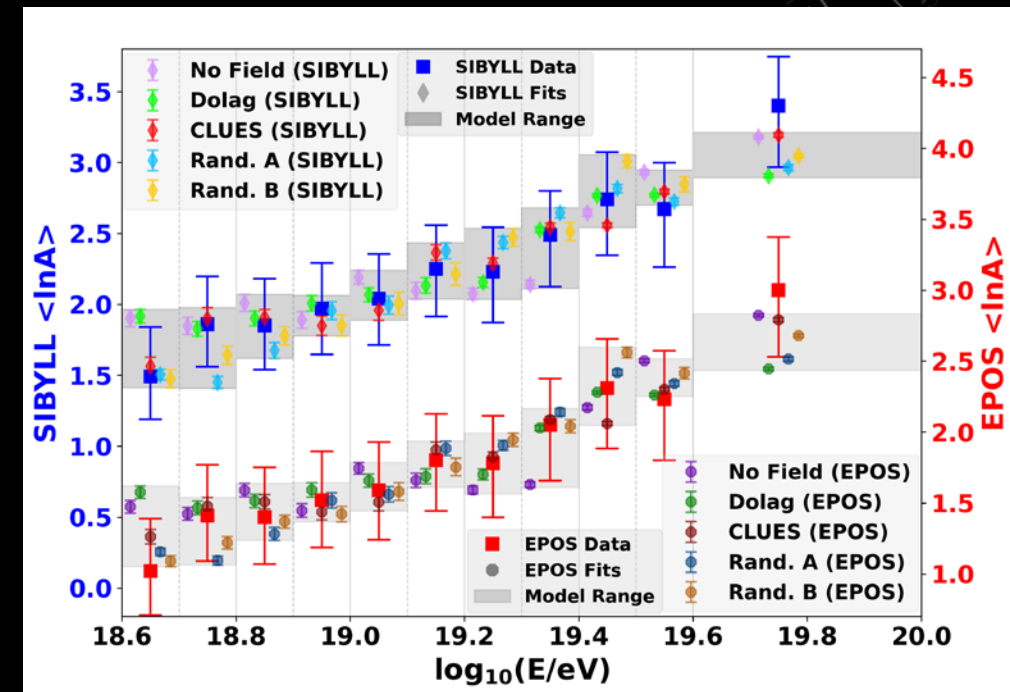
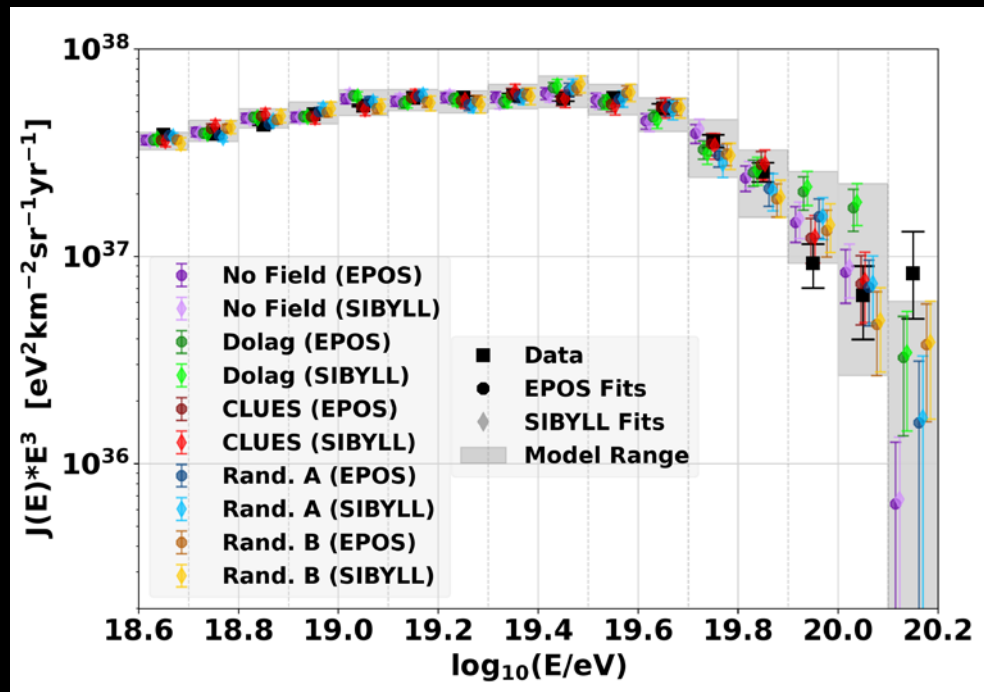
Auger JCAP (2017) [arXiv:1612.07155](https://arxiv.org/abs/1612.07155)

ENERGY SPECTRUM AND $\langle \ln A \rangle$ FITS

Data from:

Deligny, O. et al., *PoS ICRC2019 (2020) 234.*

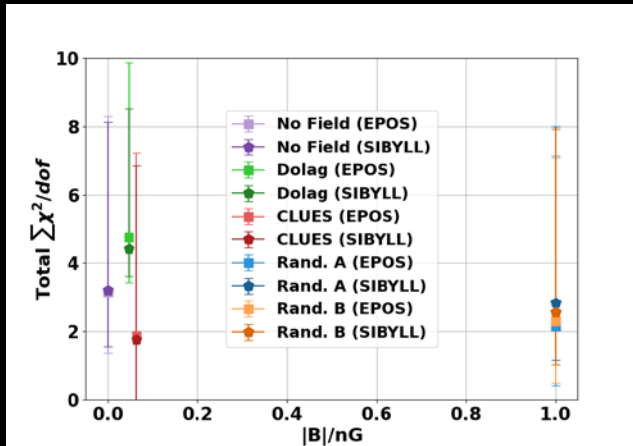
Yushkov, A. et al., *PoS ICRC2019 (2020) 482*



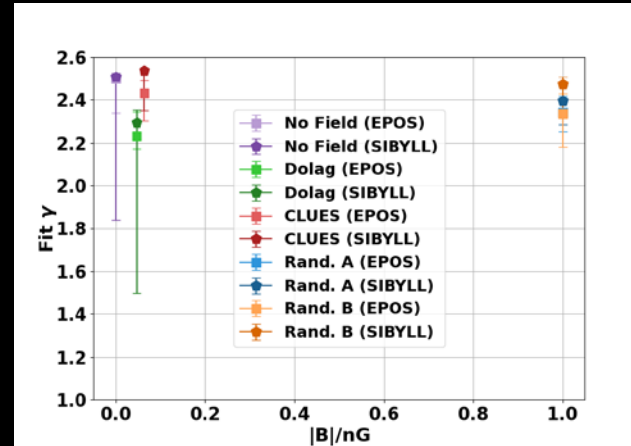
- Energy Spectra for 10 models.
- **Highest energies are not well fit.**
 - FR0 not expected as a significant contributor.
 - Contribution from other sources? SGBs? ([Abdul Halim et al. 2024](#))

- $\langle \ln A \rangle$ for 10 models.
- **Largest residuals: First and last energy bin.**

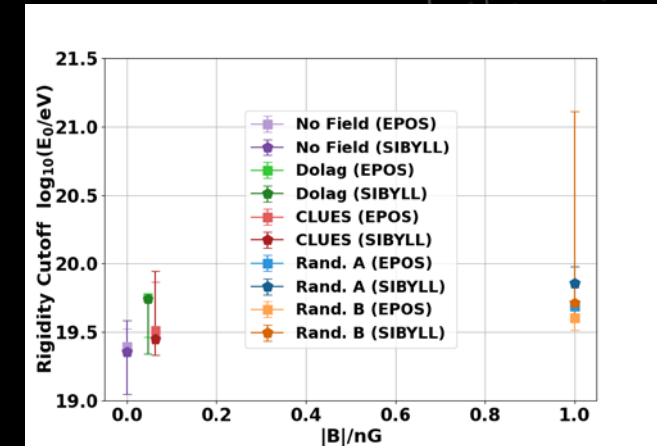
FIT PARAMETER RESULTS VS MAGNETIC FIELD



Goodness-of-fit

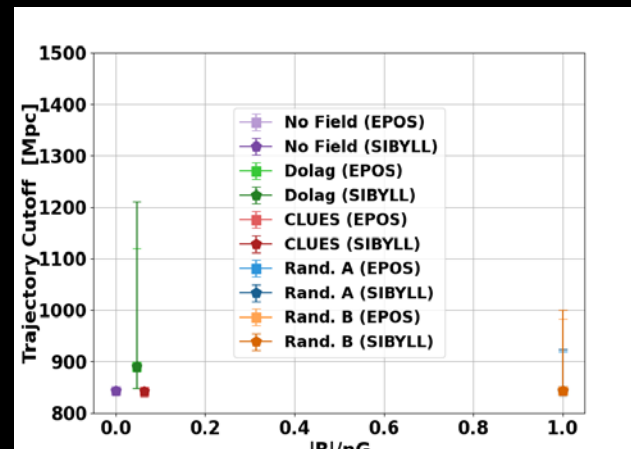


Power law Spectral Index γ

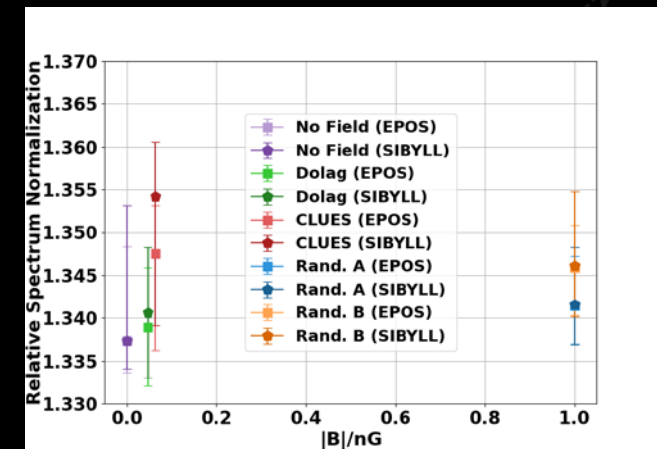


Rigidity cutoff R_{cut}

Error bars: 1 Gaussian σ C.I.
around best fit for
bootstrapped sims & data.

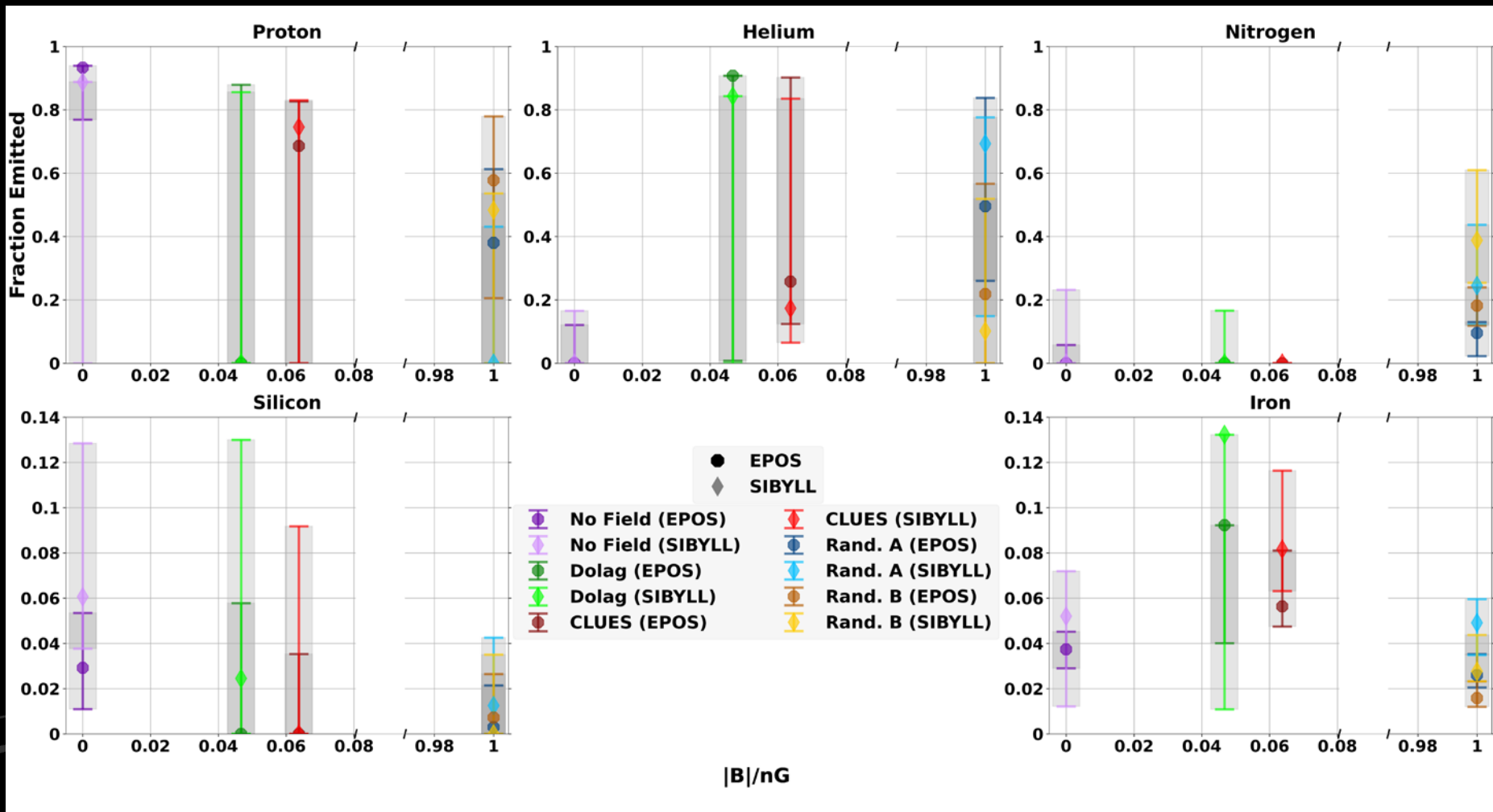


Trajectory cutoff D_{cut}



Spectrum Normalization

EMITTED NUCLEI FRACTIONS



Combined Light Nuclei

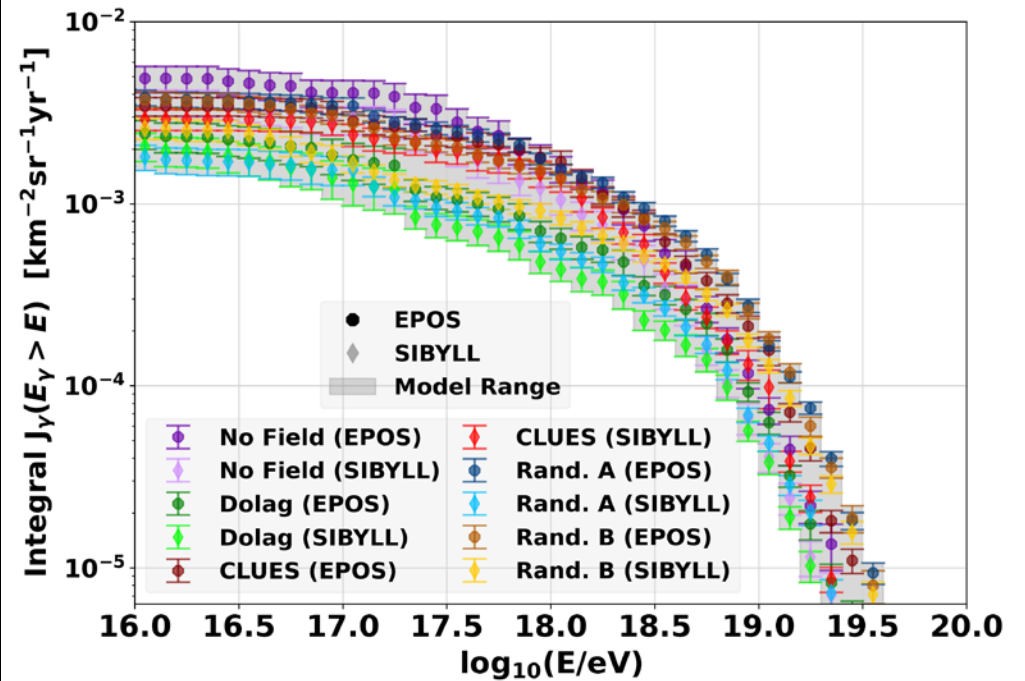
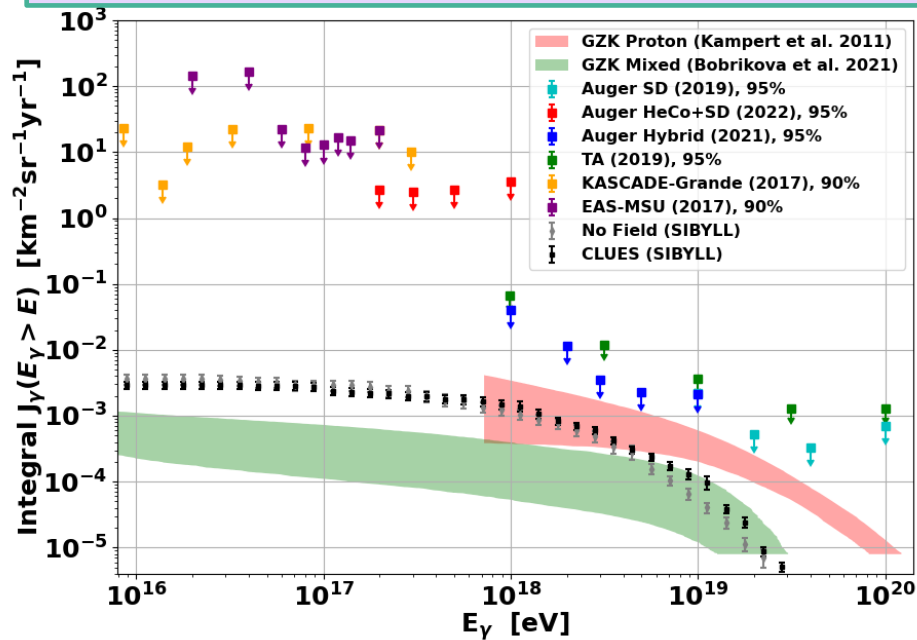
Field	Model	$f_H(\%) + f_{He}(\%)$
No Field	SIBYLL	$88.7^{+0.2}_{-24.0}$
	EPOS	$93.4^{+0.7}_{-7.2}$
	QGS4	$97.6^{+0.3}_{-1.1}$
Dolag	SIBYLL	$84.3^{+5.2}_{-11.9}$
	EPOS	$90.8^{+3.7}_{-3.8}$
	QGS4	$97.1^{+0.4}_{-1.0}$
CLUES	SIBYLL	$91.8^{+0.3}_{-11.4}$
	EPOS	$94.4^{+0.4}_{-4.4}$
	QGS4	$97.4^{+0.4}_{-0.5}$
Rand.A	SIBYLL	$69.3^{+11.1}_{-19.2}$
	EPOS	$87.6^{+5.6}_{-4.2}$
	QGS4	$98.9^{+0.0}_{-3.5}$
Rand.B	SIBYLL	$58.4^{+10.5}_{-23.6}$
	EPOS	$79.5^{+5.8}_{-6.5}$
	QGS4	$95.8^{+1.7}_{-4.5}$

Emitted Nuclei Fraction Versus Magnetic Field

PHOTONS – (CLUES-SIBYLL CONFIGURATION)

CLUES-SIBYLL

Red/green areas are no magnetic field and GZK only.



“A Search for Photons with Energies Above 2×10^{17} eV Using Hybrid Data from the Low-Energy Extensions of the Pierre Auger Observatory”

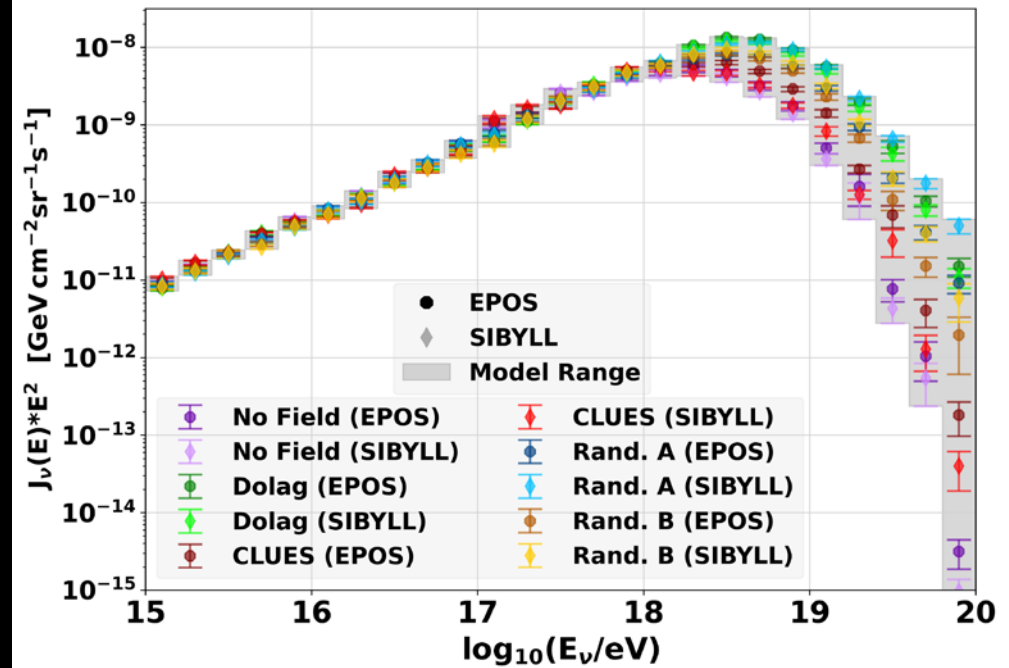
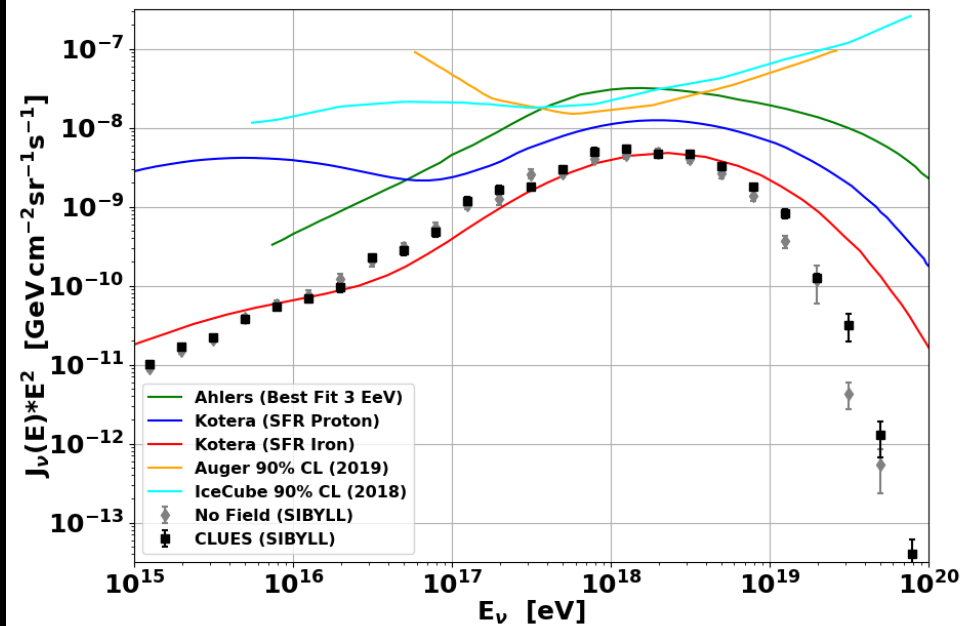
P. Abreu et al 2022 ApJ 933 125

[arXiv:2205.14864](https://arxiv.org/abs/2205.14864)

Integral photon flux for 10 models

NEUTRINOS – (CLUES-SIBYLL CONFIGURATION)

CLUES-SIBYLL



Kotera et al: JCAP (2010) [arXiv:1009.1382](https://arxiv.org/abs/1009.1382)
 Ahlers et al: Astropart.Phys.(2010) [arXiv:1005.2620v2](https://arxiv.org/abs/1005.2620v2)
 IceCube: Phys.Rev.D(2018) [arXiv:1807.01820v2](https://arxiv.org/abs/1807.01820v2)
 Auger: JCAP10 (2019) [arXiv:1906.07422v2](https://arxiv.org/abs/1906.07422v2)

Neutrino flux for 10 models

CONSTANT FRACTION CONCLUSIONS

Best Fit: CLUES Structured Field with SIBYLL EAS model.

- Next best: CLUES structured field with EPOS EAS model.
- Generally EPOS is the best fit – third: Rand.A-EPOS, fourth: Rand.B-EPOS

General trends with increasing magnetic field strength:

- Small increase: γ
- Small decrease: R_{cut}
- Increases: Helium and Nitrogen emission.
- Decreases: Proton, Silicon, and Iron emission.
- Small decrease: Proton+Helium emission.

Very good fits for CLUES and 1 nG fields with EPOS -- still may require another source type at highest energies.

Photon spectra: higher flux than expected for mixed composition from GZK only.

- Flux increases with magnetic fields at highest energies.
- Below experimental limits.

Neutrino spectra: lower flux than expected from Kotera model for mixed composition.

- Flux generally increases with magnetic fields at highest energies.
- Below experimental limits

EVOLVING FRACTION FIT



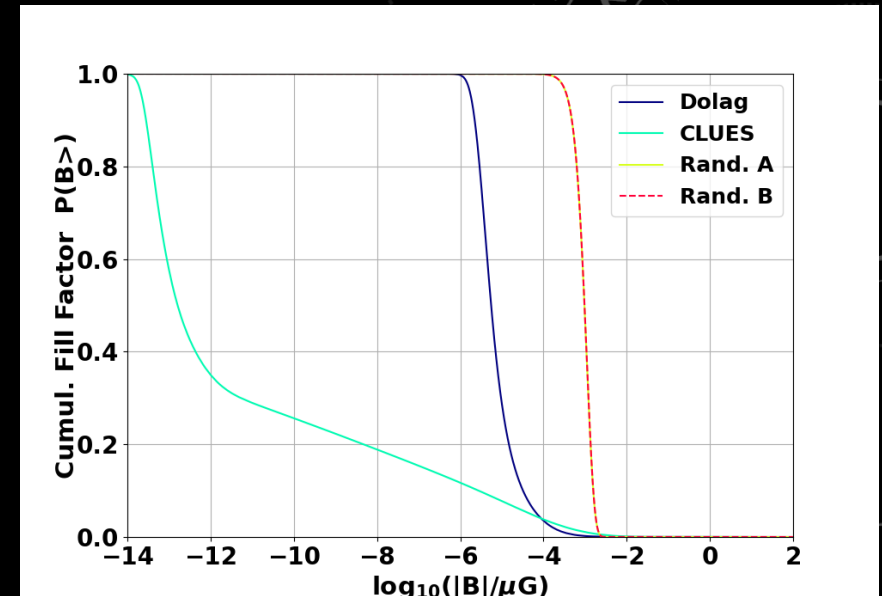
COMBINED FIT – EVOLVING FRACTIONS

- **Two EAS Models: SIBYLL2.3c, EPOS-LHC**
- **Two Structured Fields:**
 - Dolag et al. [arXiv:0410419](https://arxiv.org/abs/0410419)
 - CLUES -- Hackenstein et al. (Astro_1B): [arXiv:1710.01353](https://arxiv.org/abs/1710.01353)
- **Two 1 nG Random Fields:**
 - A: $\langle l_{\text{corr}} \rangle = 234$ kpc, B: $\langle l_{\text{corr}} \rangle = 647$ kpc
- **And no magnetic field**

$$\begin{aligned} \text{Minimize: } \sum \chi_{\text{tot}}^2 / \text{dof} &= \sum \chi_E^2 / \text{dof}_E + \sum \chi_C^2 / \text{dof}_C \\ &= \sum \chi_E^2 / 16 + \sum \chi_C^2 / 11 \end{aligned}$$

16 energy and 11 composition bins

- **48 Parameters:**
 - Power law: γ
 - Spectrum normalization: n
 - Rigidity dependent exponential cut off: ZR_{cut}
 - **5 nuclei fit:** Hydrogen, Helium, Nitrogen, Silicon, Iron.
 - Fractions sum to one – **44 parameters.**
 - Maximum trajectory D



- CRPropa3 sim. power law $\gamma = 1$
- Reweight simulated events.

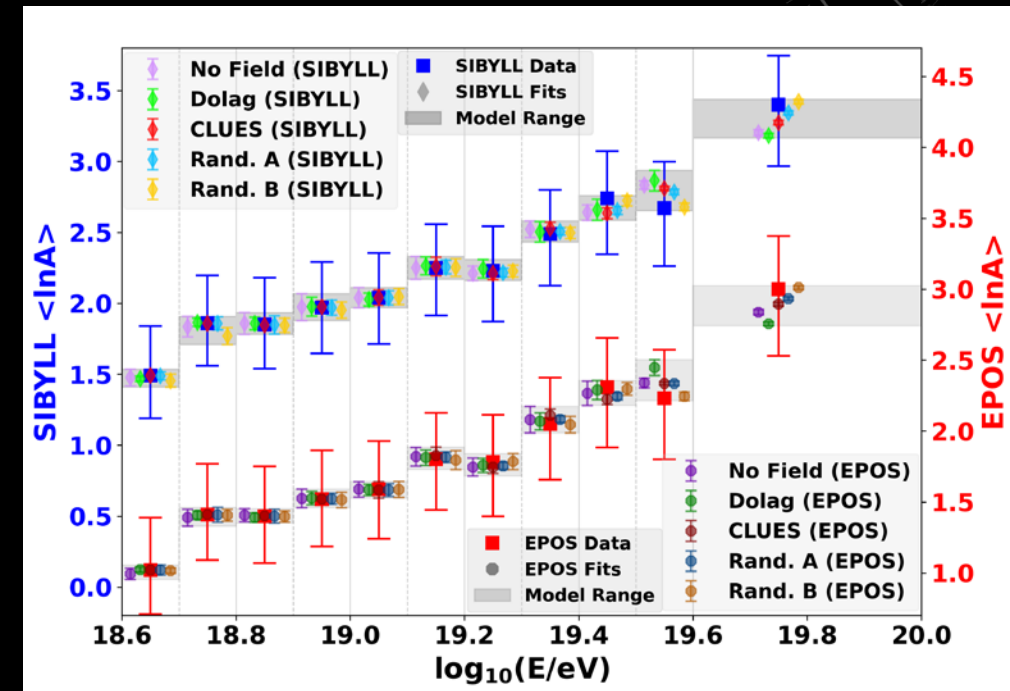
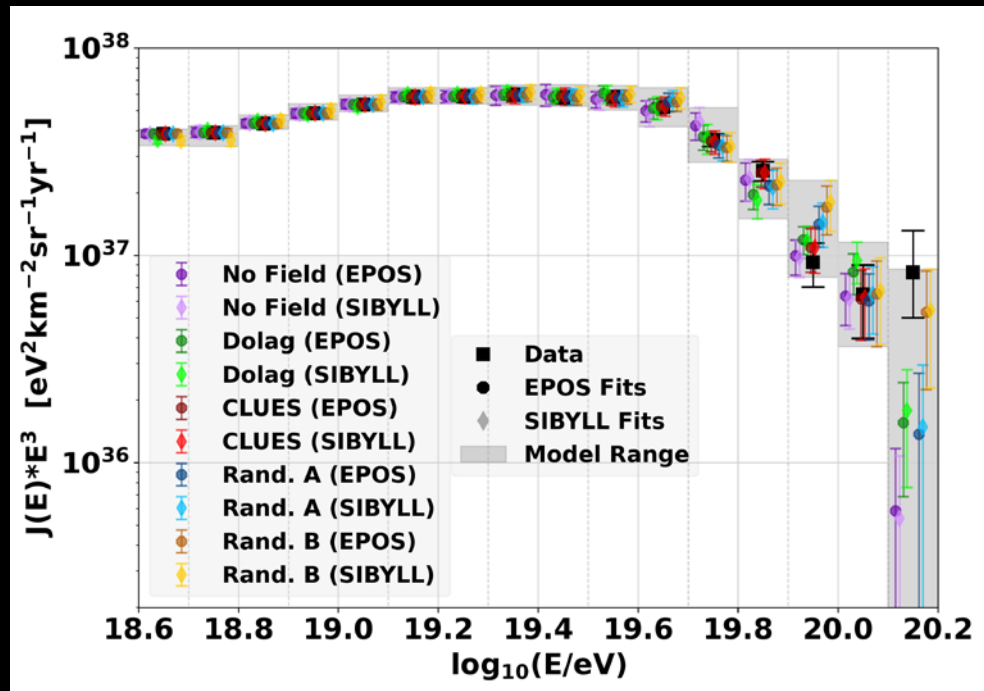
$$\frac{dN_A}{dE} = J_A(E) = f_A J_0 \left(\frac{E}{10^{18} \text{ eV}} \right)^{-\gamma} \times f_{\text{cut}}(E, Z_A R_{\text{cut}})$$

$$f_{\text{cut}}(E, Z_A R_{\text{cut}}) = \begin{cases} 1 & (E < Z_A R_{\text{cut}}) \\ \exp\left(1 - \frac{E}{Z_A R_{\text{cut}}}\right) & (E > Z_A R_{\text{cut}}) \end{cases}$$

- **Nuclei fraction: $f_A(E_{\text{obs}})$**
- Rigidity dependent cutoff: ZR_{cut}

ENERGY SPECTRUM AND $\langle \ln A \rangle$ FITS

Data from:
 Deligny, O. et al., *PoS ICRC2019 (2020) 234*.
 Yushkov, A. et al., *PoS ICRC2019 (2020) 482*

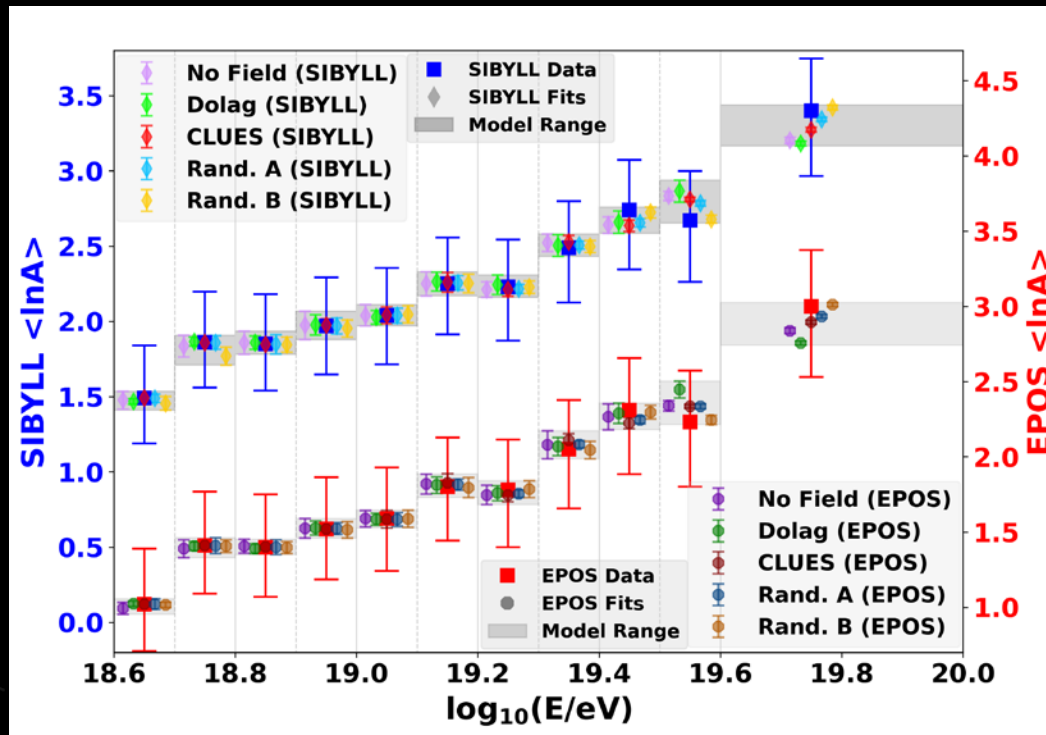


- Energy Spectra for all models.
- **Highest energy bin generally not fit.**
 - FRO perhaps not expected as a significant contributor.

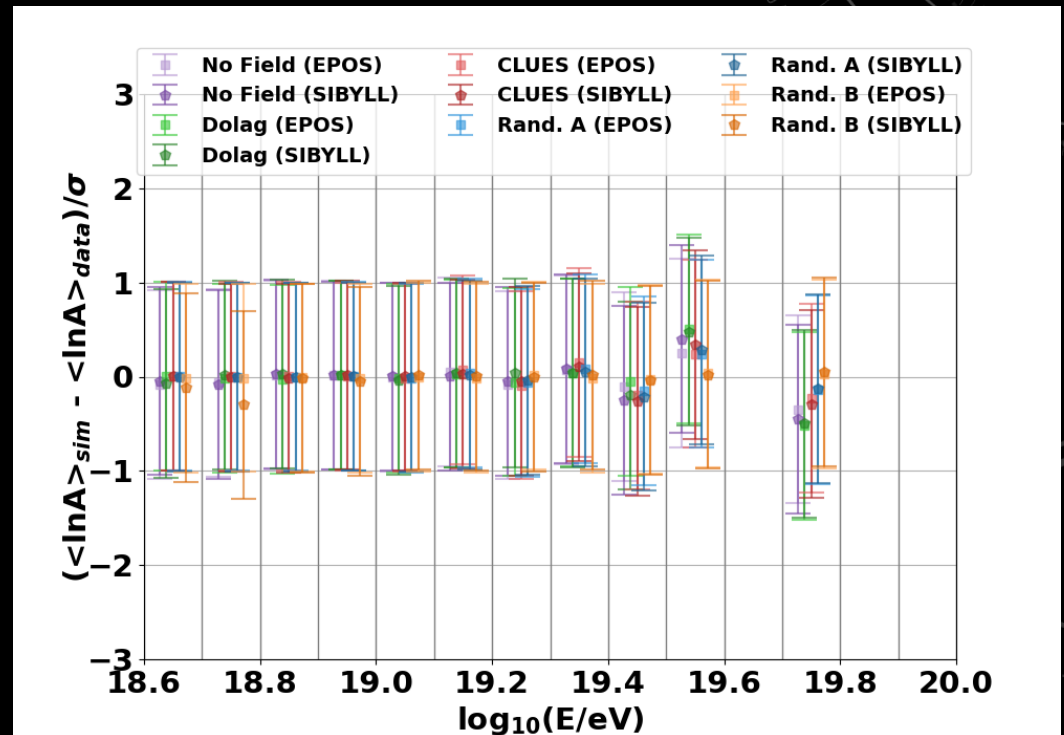
- $\langle \ln A \rangle$ for all models.
- **Very good fit. (44 parameters...)**

MEAN LOG MASS $\langle \ln A \rangle$ FITS (EVOLVING FRACTIONS)

Data From: Yushkov, A. et al., Mass Composition of Cosmic Rays with Energies above $10^{17.2}$ eV from the Hybrid Data of the Pierre Auger Observatory, *PoS ICRC2019 (2020) 482*

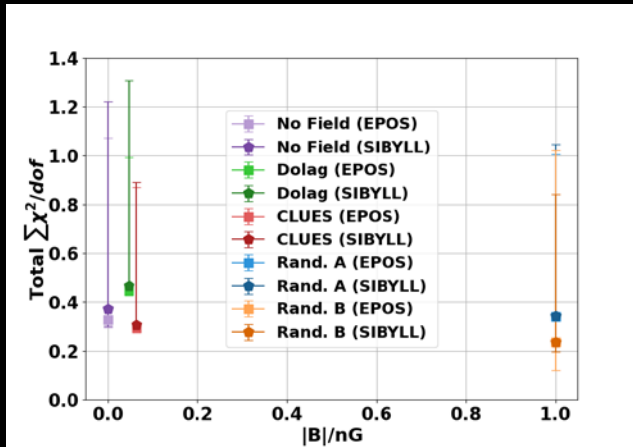


$\langle \ln A \rangle$ for all models

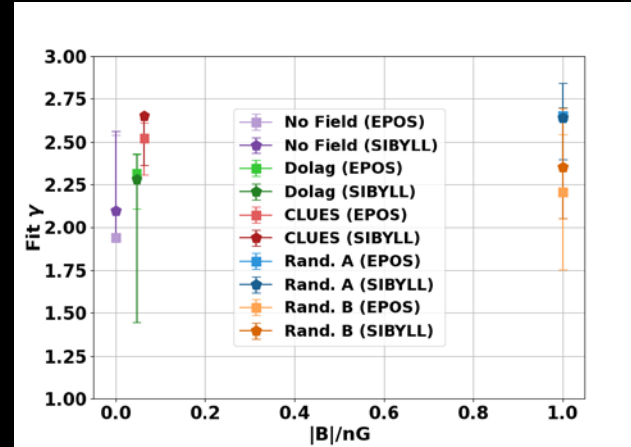


$\langle \ln A \rangle$ Residuals for all models

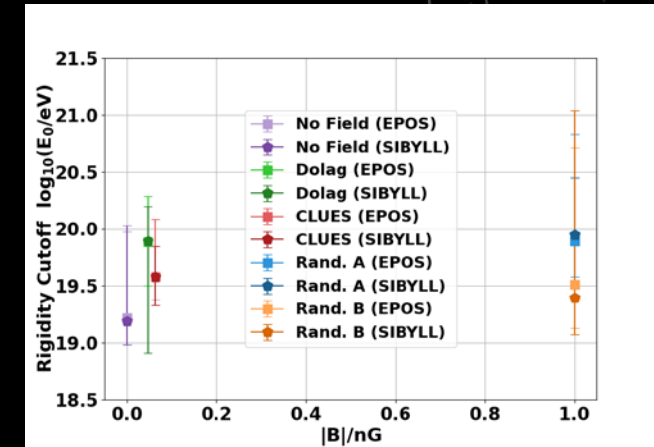
FIT PARAMETER RESULTS VS MAGNETIC FIELD



Goodness-of-fit

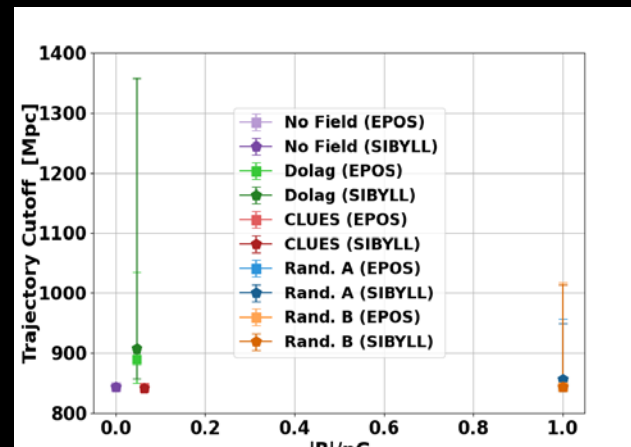


Power law Spectral Index γ

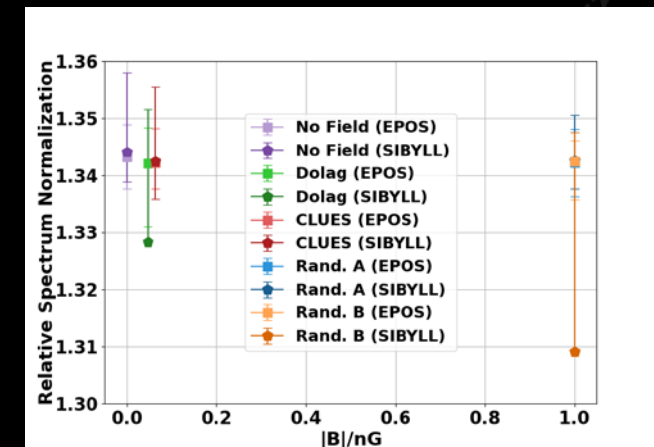


Rigidity cutoff R_{cut}

Error bars: 1 Gaussian σ C.I.
around best fit for
bootstrapped sims & data.

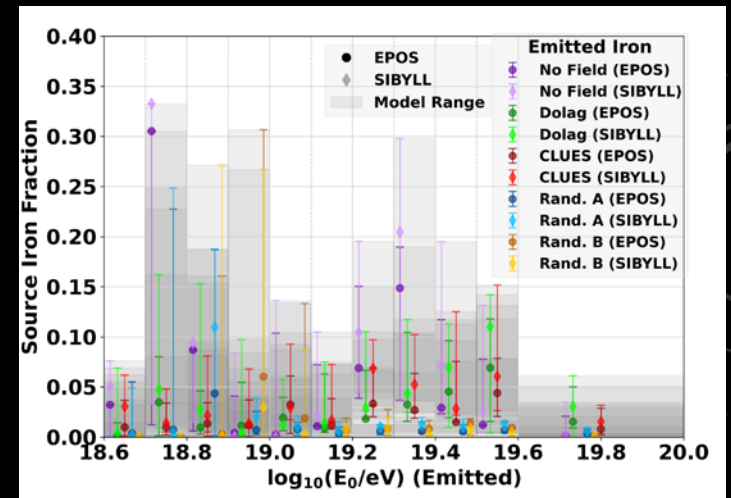
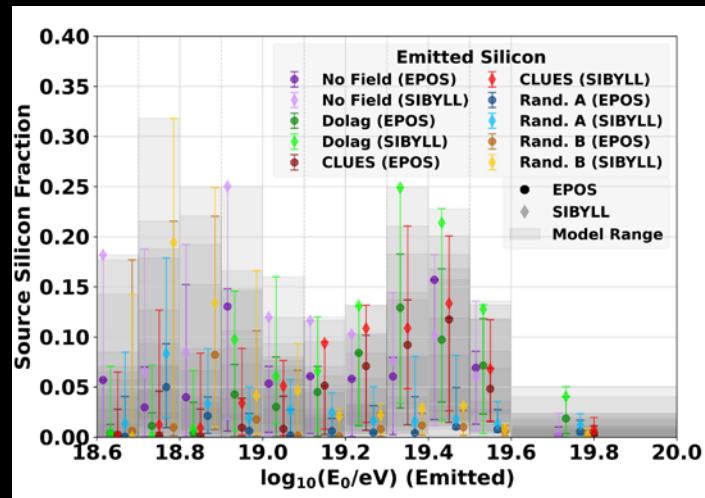
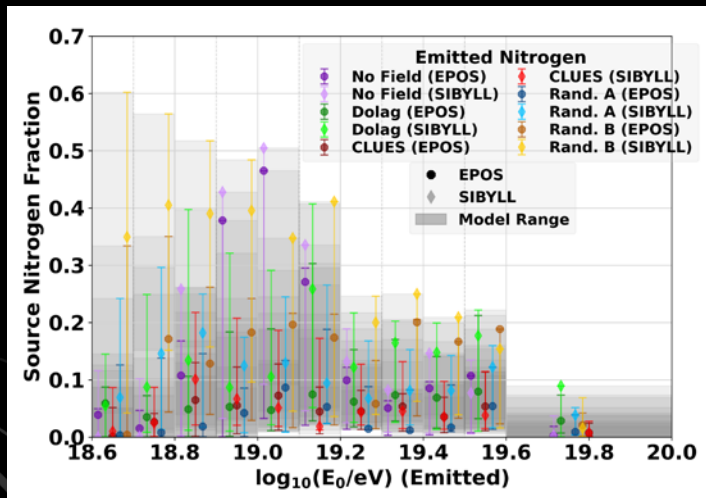
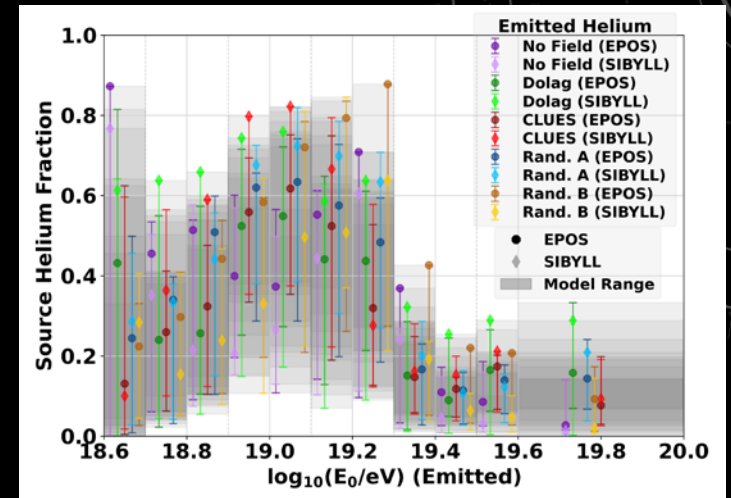
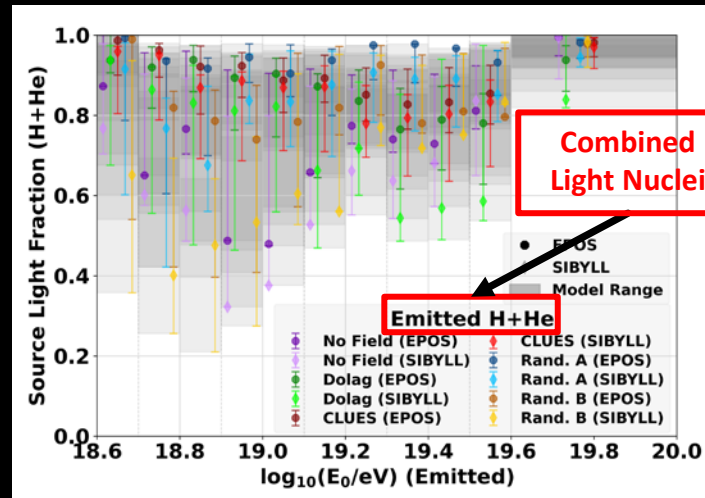
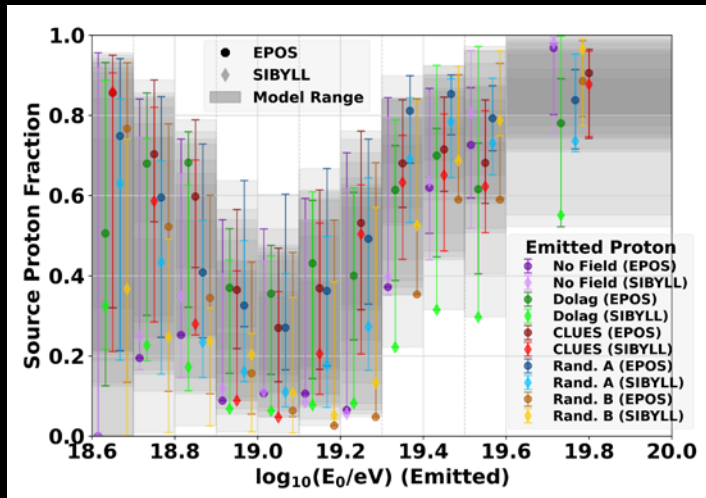


Trajectory cutoff D_{cut}



Spectrum Normalization

EVOLVING NUCLEI FRACTIONS (EMITTED)

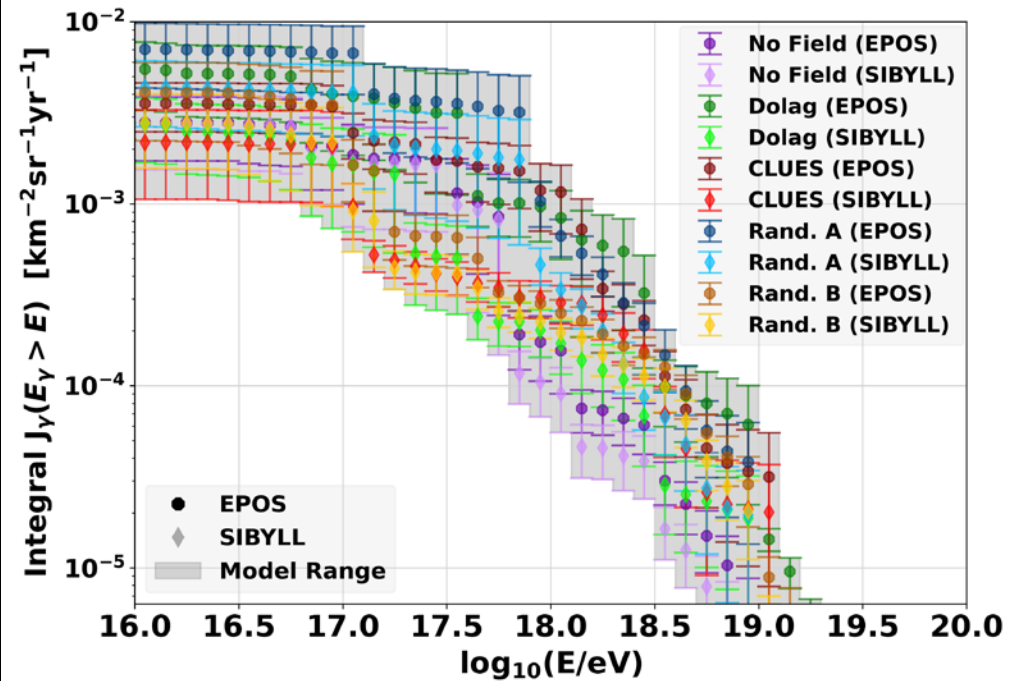
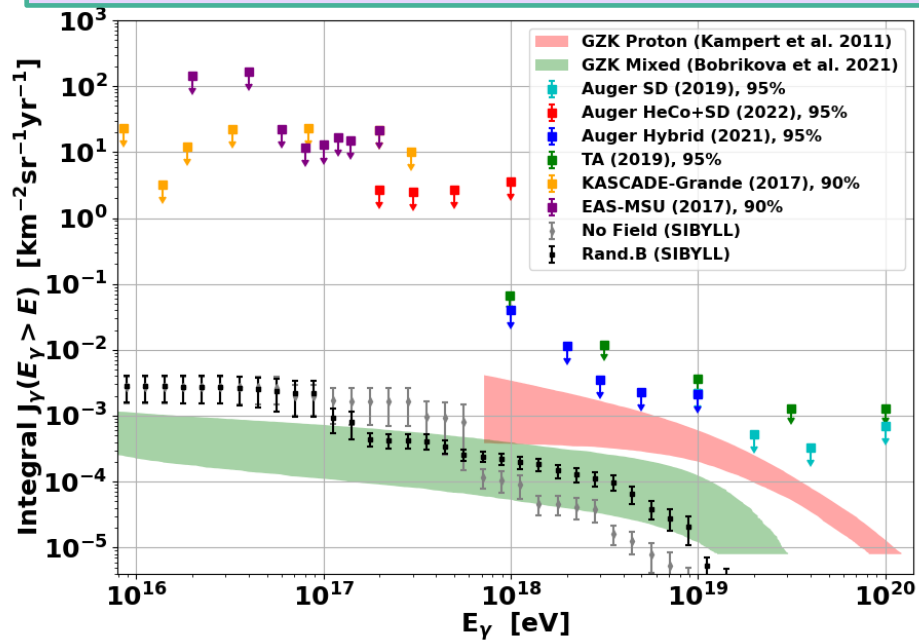


Emitted Nuclei Fraction Versus Magnetic Field

PHOTONS – (RAND.B-SIBYLL CONFIGURATION)

RAND.B-SIBYLL

Red/green areas are no magnetic field and GZK only.



“A Search for Photons with Energies Above 2×10^{17} eV Using Hybrid Data from the Low-Energy Extensions of the Pierre Auger Observatory”

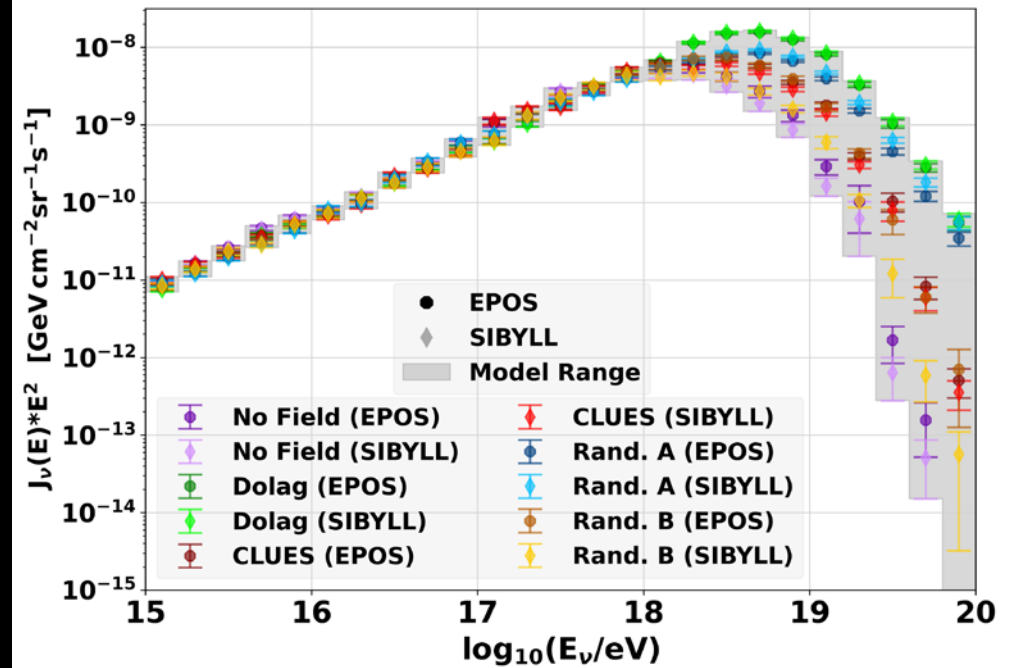
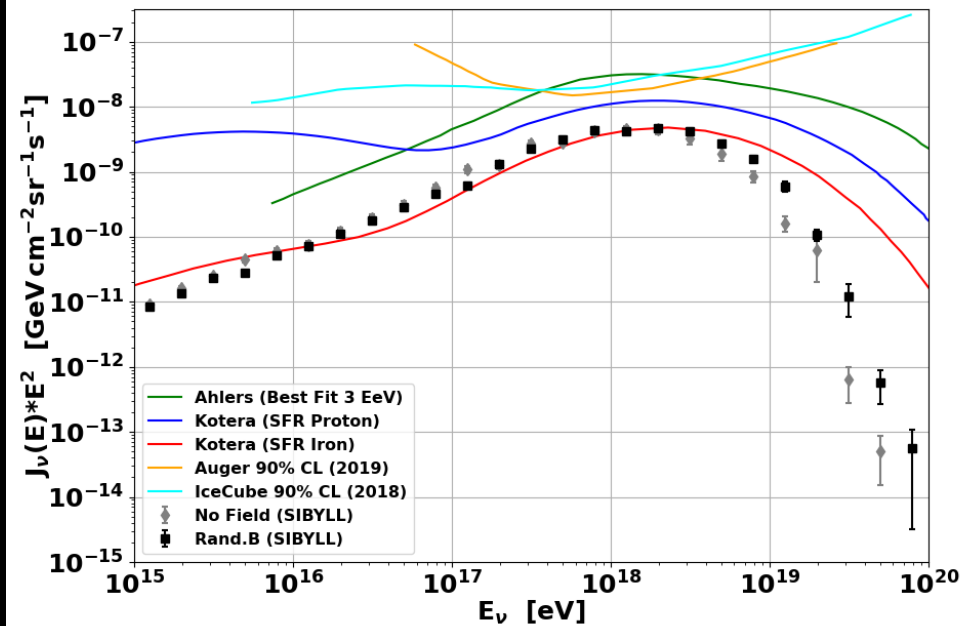
P. Abreu et al 2022 ApJ 933 125

[arXiv:2205.14864](https://arxiv.org/abs/2205.14864)

Integral photon flux for all models

NEUTRINOS – (RAND.B-SIBYLL CONFIGURATION)

RAND.B-SIBYLL



Kotera et al: JCAP (2010) [arXiv:1009.1382](https://arxiv.org/abs/1009.1382)
Ahlers et al: Astropart.Phys.(2010) [arXiv:1005.2620v2](https://arxiv.org/abs/1005.2620v2)
IceCube: Phys.Rev.D(2018) [arXiv:1807.01820v2](https://arxiv.org/abs/1807.01820v2)
Auger: JCAP10 (2019) [arXiv:1906.07422v2](https://arxiv.org/abs/1906.07422v2)

Neutrino flux for all models

EVOLVING FRACTION CONCLUSIONS

Best Fit: Rand.B 1 nG ($\langle l_{\text{corr}} \rangle = 647 \text{ kpc}$) with SIBYLL EAS model.

- Next best: Rand.B field with EPOS EAS model.
- Generally EPOS is the best fit – third: CLUES-EPOS, fourth: CLUES-SIBYLL

General trends with increasing magnetic field strength:

- Increases: γ
- Rather stable: R_{cut}

General trends with increasing energy:

- Increases: Proton emission.
- Rather stable: Light emission.
- Decreases: Heavy emission.

Extremely good fits (high parameters) still may require another source type at highest energies.

Photon spectra: consistent with mixed composition from GZK only ($E > \sim 10^{17}$).

- Flux increases with magnetic fields.
- Below experimental limits.

Neutrino spectra: lower flux than expected from Kotera model for mixed composition.

- Flux increases with magnetic fields.
- Below experimental limits.

The background features several technical diagrams. In the top right, there is a large circular gauge with concentric rings and numerical markings from 80 to 210. In the bottom right, there is a diagram with concentric circles and arrows indicating a clockwise direction. In the bottom left, there is a diagram with concentric circles and arrows indicating a counter-clockwise direction. A dark purple horizontal bar is centered across the middle of the page.

APPENDIX

The background features several technical diagrams. On the right side, there is a large circular gauge with concentric rings and numerical markings from 80 to 210. Below it is a smaller circular diagram with dashed lines and arrows. On the left side, there are partial views of similar circular diagrams. A dark purple rectangular box is centered horizontally, containing the text 'CONSTANT FRACTION ADDITIONAL' in white, bold, uppercase letters.

CONSTANT FRACTION ADDITIONAL

INTERGALACTIC PROPAGATION

CRPropa 3 used to simulate propagation of five nuclei (proton, helium, nitrogen, silicon, and iron) UHECR primaries through the intergalactic medium.

Interactions with the CMB, IRB, and URB include:

- Photo-pion production (GZK effect).
- Pair-production (including double and triple).
- Inverse Compton scattering.

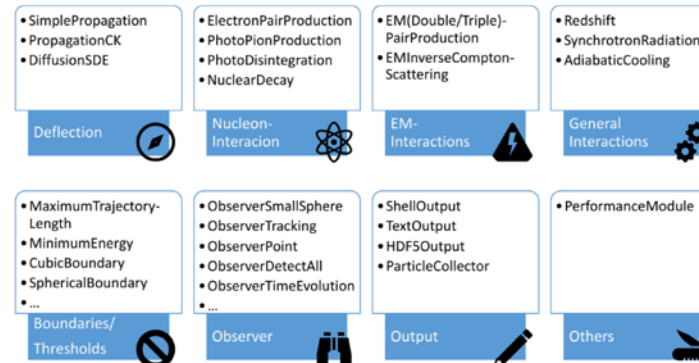
General interactions include:

- Redshift adiabatic cooling.
- Nuclear decay.

Simulation Framework **CR**Propa

Rafael Alves Batista^{a,b}, Julia Becker Tjus^c, Andrej Dundovic^a, Martin Erdmann^d, Christopher Heiter^d, Karl-Heinz Kampert^e, Daniel Kuempel^f, Lukas Merten^e, Gero Müller^d, Günter Sigl^g, Arjen van Vliet^{h,i}, David Walz^j, Tobias Winchen^{k,o}, Marcus Wirtz^d
RWTH Aachen University^d, Ruhr Universität Bochum^e, Vrije Universiteit Brussels^a, University Hamburg^g, Radboud University Nijmegen^f, University of Sao Paulo^b, Bergische Universität Wuppertal^h

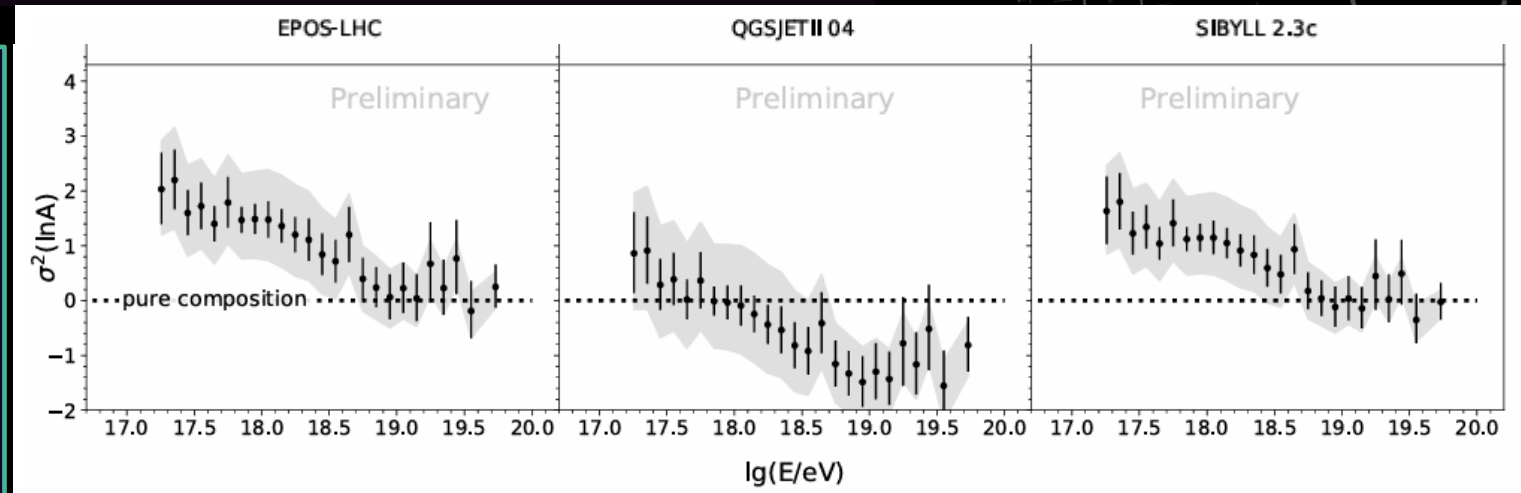
Toolbox for Simulations of UHECR Propagation



VARIANCE RESULTS

- Var(lnA) for log₁₀(E) from 18.6 to 19.0**

- No field-Sibyll: 3.38 ± 0.04
- No field-EPOS: 3.36 ± 0.07
- No field-QGS4: 2.49 ± 0.12
- Dolag-Sibyll: 2.52 ± 0.06
- Dolag-EPOS: 2.21 ± 0.08
- Dolag-QGS4: 1.71 ± 0.06
- CLUES-Sibyll: 3.29 ± 0.06
- CLUES-EPOS: 2.66 ± 0.10
- CLUES-QGS4: 1.70 ± 0.09
- 1ng1mpc-Sibyll: 1.19 ± 0.04
- 1ng1mpc-EPOS: 1.16 ± 0.05
- 1ng1mpc-QGS4: 0.66 ± 0.04
- 1ng3mpc-Sibyll: 1.23 ± 0.02
- 1ng3mpc-EPOS: 1.22 ± 0.02
- 1ng3mpc-QGS4: 0.62 ± 0.01



**Data for log₁₀(E) from 18.5 to 19.0:
 1.64 ± 0.92**

Does not include muon uncertainty
Yushkov, A. 2020, PoS, ICRC2019, 482

FIT RESULT TABLES

Field	Model	$\Sigma\chi^2/\text{dof}$	γ	$\log_{10}(R_{\text{cut}}/V)$	$D_{\text{cut}}/\text{Mpc}$	n
No Field	SIBYLL	3.21	$2.51^{+0.02}_{-0.67}$	$19.36^{+0.23}_{-0.31}$	843^{+0}_{-1}	$1.337^{+0.016}_{-0.003}$
	EPOS	3.15	$2.50^{+0.02}_{-0.16}$	$19.40^{+0.13}_{-0.06}$	843^{+0}_{-0}	$1.337^{+0.011}_{-0.004}$
	QGS4	3.47	$2.47^{+0.03}_{-0.08}$	$19.43^{+0.10}_{-0.03}$	843^{+0}_{-0}	$1.338^{+0.006}_{-0.006}$
Dolag	SIBYLL	4.41	$2.29^{+0.06}_{-0.79}$	$19.74^{+0.00}_{-0.40}$	890^{+320}_{-41}	$1.341^{+0.008}_{-0.008}$
	EPOS	4.74	$2.23^{+0.11}_{-0.06}$	$19.75^{+0.03}_{-0.29}$	889^{+230}_{-41}	$1.339^{+0.007}_{-0.007}$
	QGS4	6.28	$2.23^{+0.08}_{-0.09}$	$19.64^{+0.10}_{-0.12}$	890^{+47}_{-42}	$1.335^{+0.005}_{-0.008}$
CLUES	SIBYLL	1.76	$2.54^{+0.00}_{-0.19}$	$19.45^{+0.50}_{-0.12}$	842^{+0}_{-0}	$1.354^{+0.006}_{-0.015}$
	EPOS	1.87	$2.43^{+0.06}_{-0.13}$	$19.51^{+0.36}_{-0.07}$	842^{+0}_{-1}	$1.347^{+0.006}_{-0.011}$
	QGS4	3.10	$2.32^{+0.08}_{-0.05}$	$19.56^{+0.08}_{-0.07}$	841^{+1}_{-0}	$1.334^{+0.006}_{-0.007}$
Rand.A	SIBYLL	2.84	$2.40^{+0.07}_{-0.11}$	$19.86^{+0.12}_{-0.18}$	843^{+80}_{-0}	$1.342^{+0.007}_{-0.005}$
	EPOS	2.15	$2.34^{+0.08}_{-0.09}$	$19.69^{+0.19}_{-0.08}$	843^{+76}_{-0}	$1.341^{+0.006}_{-0.004}$
	QGS4	2.51	$2.23^{+0.07}_{-0.07}$	$19.58^{+0.07}_{-0.08}$	846^{+69}_{-0}	$1.341^{+0.005}_{-0.006}$
Rand.B	SIBYLL	2.57	$2.47^{+0.04}_{-0.16}$	$19.71^{+1.40}_{-0.08}$	843^{+156}_{-0}	$1.346^{+0.009}_{-0.006}$
	EPOS	2.29	$2.33^{+0.09}_{-0.15}$	$19.60^{+0.23}_{-0.09}$	843^{+140}_{-0}	$1.346^{+0.005}_{-0.006}$
	QGS4	2.60	$1.97^{+0.26}_{-0.05}$	$19.52^{+0.08}_{-0.07}$	854^{+66}_{-11}	$1.343^{+0.006}_{-0.004}$

Table 1: The FR0 combined fit results total sum chi-square per degree of freedom, spectral index γ , exponential rigidity cutoff ($\log_{10}(R_{\text{cut}})$), trajectory cutoff (D_{cut}), and spectrum normalization for all 15 models. The three extensive air-shower models are EPOS-LHC (EPOS), Sibyll2.3c (SIBYLL), and QGSJetII-04 (QGS4).

FIT RESULT TABLES

Field	Model	$f_H(\%) + f_{He}(\%)$	$f_H(\%)$	$f_{He}(\%)$	$f_N(\%)$	$f_{Si}(\%)$	$f_{Fe}(\%)$
No Field	SIBYLL	$88.7^{+0.2}_{-24.0}$	$88.7^{+0.1}_{-88.7}$	$0.0^{+16.5}_{-0.0}$	$0.0^{+23.1}_{-0.0}$	$6.1^{+6.8}_{-2.3}$	$5.2^{+2.0}_{-4.0}$
	EPOS	$93.4^{+0.7}_{-7.2}$	$93.4^{+0.6}_{-16.5}$	$0.0^{+12.1}_{-0.0}$	$0.0^{+5.8}_{-0.0}$	$2.9^{+2.4}_{-1.8}$	$3.7^{+0.8}_{-0.8}$
	QGS4	$97.6^{+0.3}_{-1.1}$	$97.6^{+0.1}_{-8.8}$	$0.0^{+7.8}_{-0.0}$	$0.0^{+0.0}_{-0.0}$	$0.2^{+1.2}_{-0.2}$	$2.2^{+0.2}_{-0.5}$
Dolag	SIBYLL	$84.3^{+5.2}_{-11.9}$	$0.0^{+85.6}_{-0.0}$	$84.3^{+0.0}_{-84.3}$	$0.0^{+16.6}_{-0.0}$	$2.5^{+10.5}_{-2.4}$	$13.2^{+0.0}_{-12.1}$
	EPOS	$90.8^{+3.7}_{-3.8}$	$0.0^{+87.9}_{-0.0}$	$90.8^{+0.0}_{-90.0}$	$0.0^{+0.0}_{-0.0}$	$0.0^{+5.8}_{-0.0}$	$9.2^{+0.0}_{-5.2}$
	QGS4	$97.1^{+0.4}_{-1.0}$	$54.4^{+28.3}_{-35.4}$	$42.7^{+34.7}_{-28.4}$	$0.0^{+0.0}_{-0.0}$	$0.0^{+0.0}_{-0.0}$	$2.9^{+0.9}_{-0.5}$
CLUES	SIBYLL	$91.8^{+0.3}_{-11.4}$	$74.5^{+8.5}_{-74.5}$	$17.3^{+66.2}_{-10.8}$	$0.0^{+0.0}_{-0.0}$	$0.0^{+9.2}_{-0.0}$	$8.2^{+3.5}_{-1.8}$
	EPOS	$94.4^{+0.4}_{-4.4}$	$68.6^{+14.1}_{-68.6}$	$25.8^{+64.4}_{-13.4}$	$0.0^{+0.0}_{-0.0}$	$0.0^{+3.5}_{-0.0}$	$5.6^{+2.5}_{-0.9}$
	QGS4	$97.4^{+0.4}_{-0.5}$	$68.8^{+16.3}_{-15.8}$	$28.6^{+15.6}_{-16.1}$	$0.0^{+0.0}_{-0.0}$	$0.0^{+0.0}_{-0.0}$	$2.6^{+0.5}_{-0.4}$
Rand.A	SIBYLL	$69.3^{+11.1}_{-19.2}$	$0.0^{+43.1}_{-0.0}$	$69.3^{+8.3}_{-54.4}$	$24.5^{+19.2}_{-12.3}$	$1.3^{+3.0}_{-1.3}$	$4.9^{+1.0}_{-1.4}$
	EPOS	$87.6^{+5.6}_{-4.2}$	$38.0^{+23.3}_{-38.0}$	$49.6^{+34.2}_{-23.5}$	$9.5^{+3.5}_{-7.3}$	$0.3^{+1.8}_{-0.3}$	$2.6^{+0.9}_{-0.5}$
	QGS4	$98.9^{+0.0}_{-3.5}$	$57.9^{+18.4}_{-12.1}$	$41.0^{+10.0}_{-20.7}$	$0.0^{+3.5}_{-0.0}$	$0.0^{+0.1}_{-0.0}$	$1.1^{+0.2}_{-0.2}$
Rand.B	SIBYLL	$58.4^{+10.5}_{-23.6}$	$48.3^{+5.3}_{-48.3}$	$10.1^{+41.8}_{-10.1}$	$38.8^{+22.2}_{-13.4}$	$0.0^{+3.5}_{-0.0}$	$2.8^{+1.6}_{-0.4}$
	EPOS	$79.5^{+5.8}_{-6.5}$	$57.7^{+20.2}_{-37.2}$	$21.8^{+34.9}_{-21.8}$	$18.2^{+5.8}_{-6.3}$	$0.7^{+1.9}_{-0.7}$	$1.6^{+0.7}_{-0.4}$
	QGS4	$95.8^{+1.7}_{-4.5}$	$45.6^{+41.0}_{-9.4}$	$50.2^{+9.0}_{-43.1}$	$2.2^{+5.1}_{-2.2}$	$0.9^{+0.6}_{-0.9}$	$1.1^{+0.2}_{-0.4}$

Table 3: The FR0 combined fit nuclei emission percentages for proton, helium, nitrogen, silicon, and iron primaries for all 15 models.

FIT RESULT TABLES

Table 2. Constant Fraction Bootstrap Energy Spectrum Parameters

Field	Model	$\Sigma\chi^2/\text{dof}$	γ	$\log_{10}(R_{\text{cut}}/V)$	$D_{\text{cut}}/\text{Mpc}$	n
No Field	SIBYLL	3.21	$2.48^{+0.27}_{-0.27}$	$19.38^{+0.23}_{-0.23}$	843^{+0}_{-0}	$1.341^{+0.006}_{-0.006}$
	EPOS	3.15	$2.48^{+0.26}_{-0.26}$	$19.40^{+0.13}_{-0.13}$	843^{+0}_{-0}	$1.338^{+0.005}_{-0.005}$
	QGS4	3.47	$2.45^{+0.04}_{-0.04}$	$19.43^{+0.06}_{-0.06}$	843^{+0}_{-0}	$1.335^{+0.004}_{-0.004}$
Dolag	SIBYLL	4.41	$2.07^{+0.23}_{-0.23}$	$19.04^{+0.57}_{-0.57}$	871^{+126}_{-29}	$1.339^{+0.005}_{-0.005}$
	EPOS	4.74	$2.33^{+0.38}_{-0.38}$	$19.37^{+0.24}_{-0.24}$	864^{+180}_{-22}	$1.334^{+0.004}_{-0.004}$
	QGS4	6.28	$2.24^{+0.37}_{-0.37}$	$19.64^{+0.07}_{-0.07}$	893^{+86}_{-51}	$1.335^{+0.004}_{-0.004}$
CLUES	SIBYLL	1.76	$2.54^{+0.15}_{-0.15}$	$19.41^{+0.34}_{-0.34}$	842^{+0}_{-0}	$1.352^{+0.007}_{-0.007}$
	EPOS	1.87	$2.41^{+0.07}_{-0.07}$	$19.51^{+0.15}_{-0.15}$	842^{+0}_{-0}	$1.346^{+0.005}_{-0.005}$
	QGS4	3.10	$2.31^{+0.05}_{-0.05}$	$19.56^{+0.06}_{-0.06}$	842^{+0}_{-0}	$1.337^{+0.004}_{-0.004}$
Rand.A	SIBYLL	2.84	$2.36^{+0.26}_{-0.26}$	$19.87^{+1.66}_{-1.66}$	864^{+81}_{-22}	$1.343^{+0.001}_{-0.001}$
	EPOS	2.15	$2.31^{+0.05}_{-0.05}$	$19.67^{+0.11}_{-0.11}$	853^{+36}_{-11}	$1.343^{+0.003}_{-0.003}$
	QGS4	2.51	$2.25^{+0.07}_{-0.07}$	$19.59^{+0.08}_{-0.08}$	854^{+29}_{-12}	$1.342^{+0.004}_{-0.004}$
Rand.B	SIBYLL	2.57	$2.43^{+0.06}_{-0.06}$	$19.70^{+10.20}_{-10.20}$	852^{+53}_{-10}	$1.347^{+0.005}_{-0.005}$
	EPOS	2.29	$2.36^{+0.10}_{-0.10}$	$19.54^{+7.2}_{-7.2}$	854^{+64}_{-12}	$1.346^{+0.000}_{-0.000}$
	QGS4	2.60	$2.15^{+0.14}_{-0.14}$	$19.45^{+0.62}_{-0.62}$	848^{+48}_{-6}	$1.342^{+0.003}_{-0.003}$

Notes. The FR0 constant fraction combined fit bootstrap distribution most probable spectral index γ , exponential rigidity cutoff ($\log_{10}(R_{\text{cut}}/V)$), trajectory cutoff (D_{cut}), and spectrum normalization for all 15 configurations.

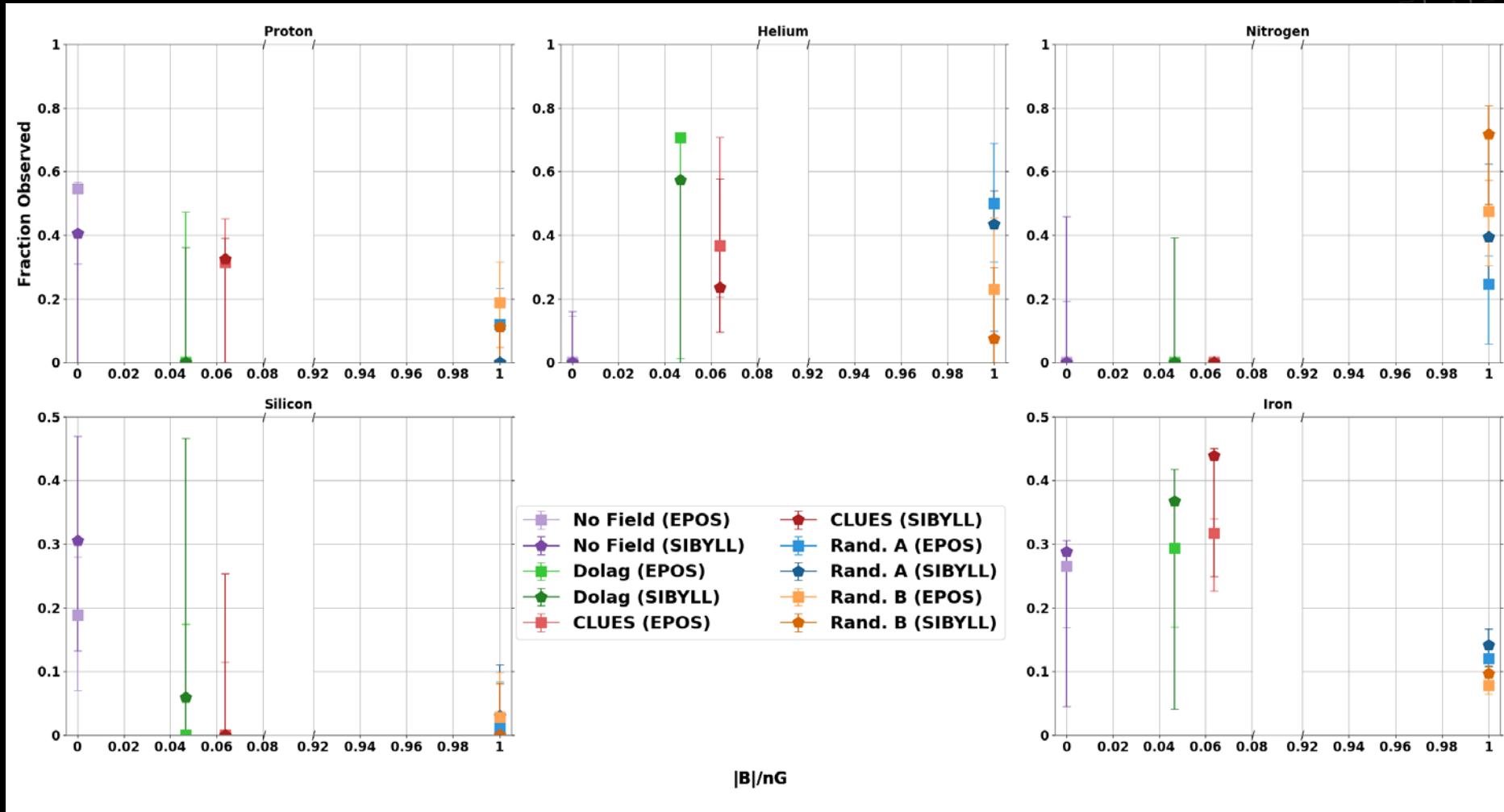
FIT RESULT TABLES

Table 4. Constant Fraction Bootstrap Composition Parameters

Field	Model	$f_H(\%) + f_{He}(\%)$	$f_H(\%)$	$f_{He}(\%)$	$f_N(\%)$	$f_{Si}(\%)$	$f_{Fe}(\%)$
No Field	SIBYLL	$86.3^{+13.7}_{-15.6}$	$85.6^{+14.4}_{-21.7}$	$0.6^{+15.2}_{-0.6}$	$2.8^{+15.8}_{-2.8}$	$5.6^{+3.1}_{-3.1}$	$5.4^{+2.3}_{-2.3}$
	EPOS	$92.8^{+5.3}_{-5.3}$	$91.4^{+8.6}_{-13.2}$	$1.4^{+10.7}_{-1.4}$	$0.6^{+5.3}_{-0.6}$	$2.9^{+1.5}_{-1.5}$	$3.7^{+0.8}_{-0.8}$
	QGS4	$97.6^{+0.8}_{-0.8}$	$96.4^{+3.6}_{-7.6}$	$1.2^{+7.4}_{-1.2}$	$0.0^{+0.8}_{-0.0}$	$0.2^{+0.5}_{-0.2}$	$2.2^{+0.2}_{-0.2}$
Dolag	SIBYLL	$85.2^{+8.0}_{-8.0}$	$84.4^{+15.6}_{-22.6}$	$0.9^{+22.1}_{-0.9}$	$0.0^{+7.6}_{-0.0}$	$13.0^{+3.9}_{-3.9}$	$1.8^{+3.1}_{-1.8}$
	EPOS	$94.8^{+4.9}_{-4.9}$	$84.5^{+15.5}_{-23.6}$	$10.3^{+22.4}_{-10.3}$	$0.1^{+4.7}_{-0.1}$	$0.2^{+2.2}_{-0.2}$	$4.9^{+1.7}_{-1.7}$
	QGS4	$97.0^{+0.6}_{-0.6}$	$54.7^{+18.0}_{-18.0}$	$42.3^{+17.7}_{-17.7}$	$0.0^{+0.5}_{-0.0}$	$0.0^{+0.3}_{-0.0}$	$2.9^{+0.5}_{-0.5}$
CLUES	SIBYLL	$91.6^{+3.6}_{-3.6}$	$81.2^{+18.8}_{-23.3}$	$10.6^{+20.7}_{-10.6}$	$0.0^{+2.2}_{-0.0}$	$0.7^{+3.4}_{-0.7}$	$7.5^{+1.9}_{-1.9}$
	EPOS	$94.2^{+1.8}_{-1.8}$	$66.7^{+21.8}_{-21.8}$	$27.6^{+20.5}_{-20.5}$	$0.0^{+0.5}_{-0.0}$	$0.2^{+1.6}_{-0.2}$	$5.5^{+1.0}_{-1.0}$
	QGS4	$97.5^{+0.4}_{-0.4}$	$67.6^{+12.3}_{-12.3}$	$29.9^{+12.1}_{-12.1}$	$0.0^{+0.0}_{-0.0}$	$0.0^{+0.2}_{-0.0}$	$2.5^{+0.3}_{-0.3}$
Rand.A	SIBYLL	$70.0^{+11.4}_{-11.4}$	$5.3^{+14.7}_{-5.3}$	$63.9^{+17.5}_{-17.5}$	$25.1^{+11.8}_{-11.8}$	$0.7^{+1.5}_{-0.7}$	$5.0^{+0.9}_{-0.9}$
	EPOS	$87.6^{+4.6}_{-4.6}$	$36.2^{+15.9}_{-15.9}$	$51.5^{+16.0}_{-16.0}$	$9.5^{+4.9}_{-4.9}$	$0.2^{+0.8}_{-0.2}$	$2.7^{+0.5}_{-0.5}$
	QGS4	$98.4^{+1.1}_{-1.1}$	$60.6^{+10.1}_{-10.1}$	$37.7^{+10.4}_{-10.4}$	$0.5^{+1.2}_{-0.5}$	$0.0^{+0.2}_{-0.0}$	$1.1^{+0.2}_{-0.2}$
Rand.B	SIBYLL	$59.3^{+11.1}_{-11.1}$	$45.7^{+15.3}_{-15.3}$	$15.2^{+14.4}_{-14.4}$	$35.8^{+11.5}_{-11.5}$	$0.6^{+1.3}_{-0.6}$	$2.7^{+0.6}_{-0.6}$
	EPOS	$82.0^{+4.5}_{-4.5}$	$73.3^{+16.3}_{-16.3}$	$9.5^{+14.8}_{-9.5}$	$15.6^{+4.7}_{-4.7}$	$0.2^{+1.0}_{-0.2}$	$1.4^{+0.4}_{-0.4}$
	QGS4	$93.6^{+1.8}_{-1.8}$	$80.4^{+14.2}_{-14.2}$	$13.2^{+14.7}_{-13.2}$	$5.6^{+2.1}_{-2.1}$	$0.0^{+0.4}_{-0.0}$	$0.7^{+0.2}_{-0.2}$

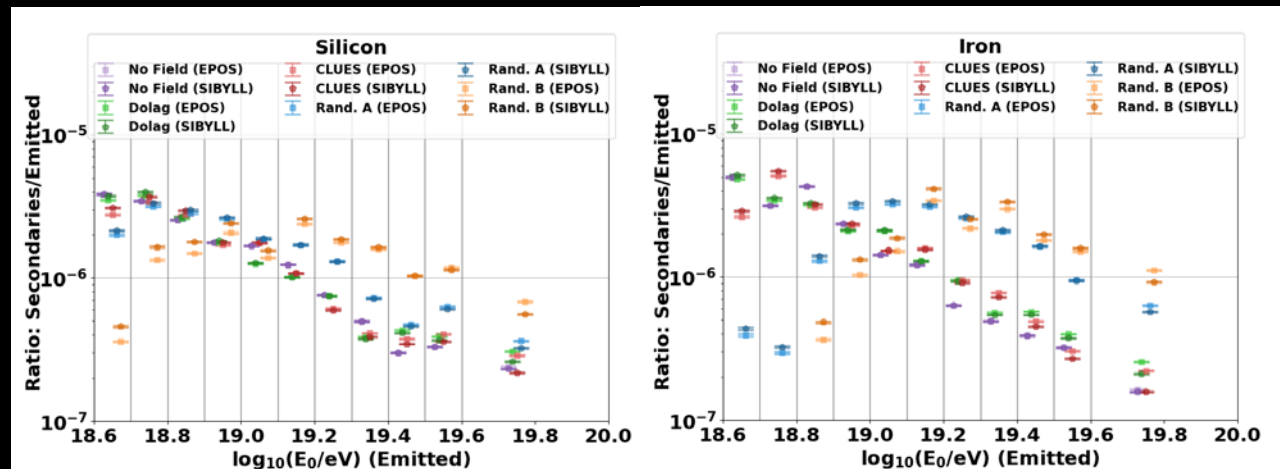
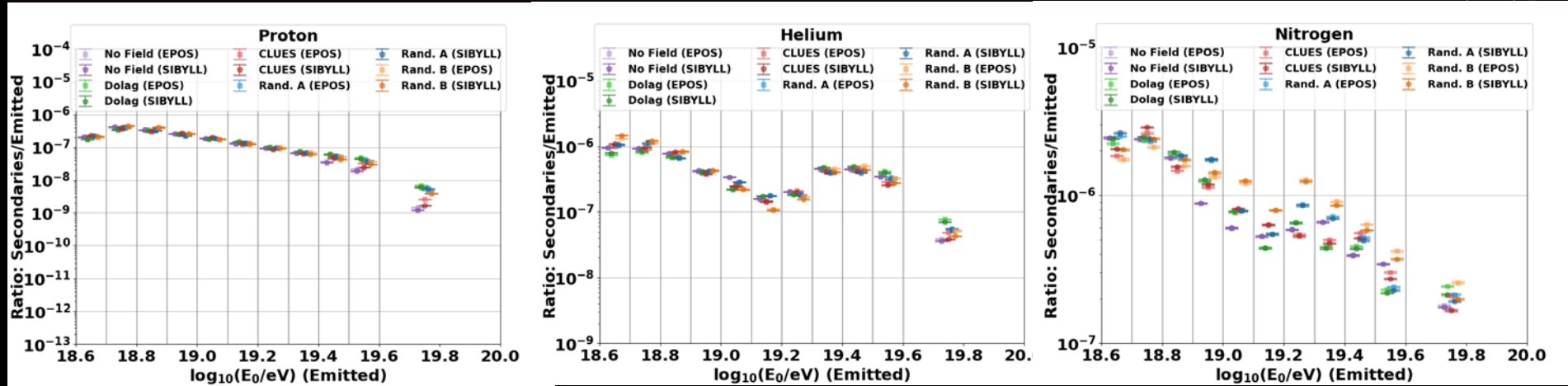
Notes. The FR0 constant fraction combined fit bootstrap distribution most probable nuclei emission percentages for proton, helium, nitrogen, silicon, and iron primaries for all 15 configurations.

OBSERVED NUCLEI FRACTIONS



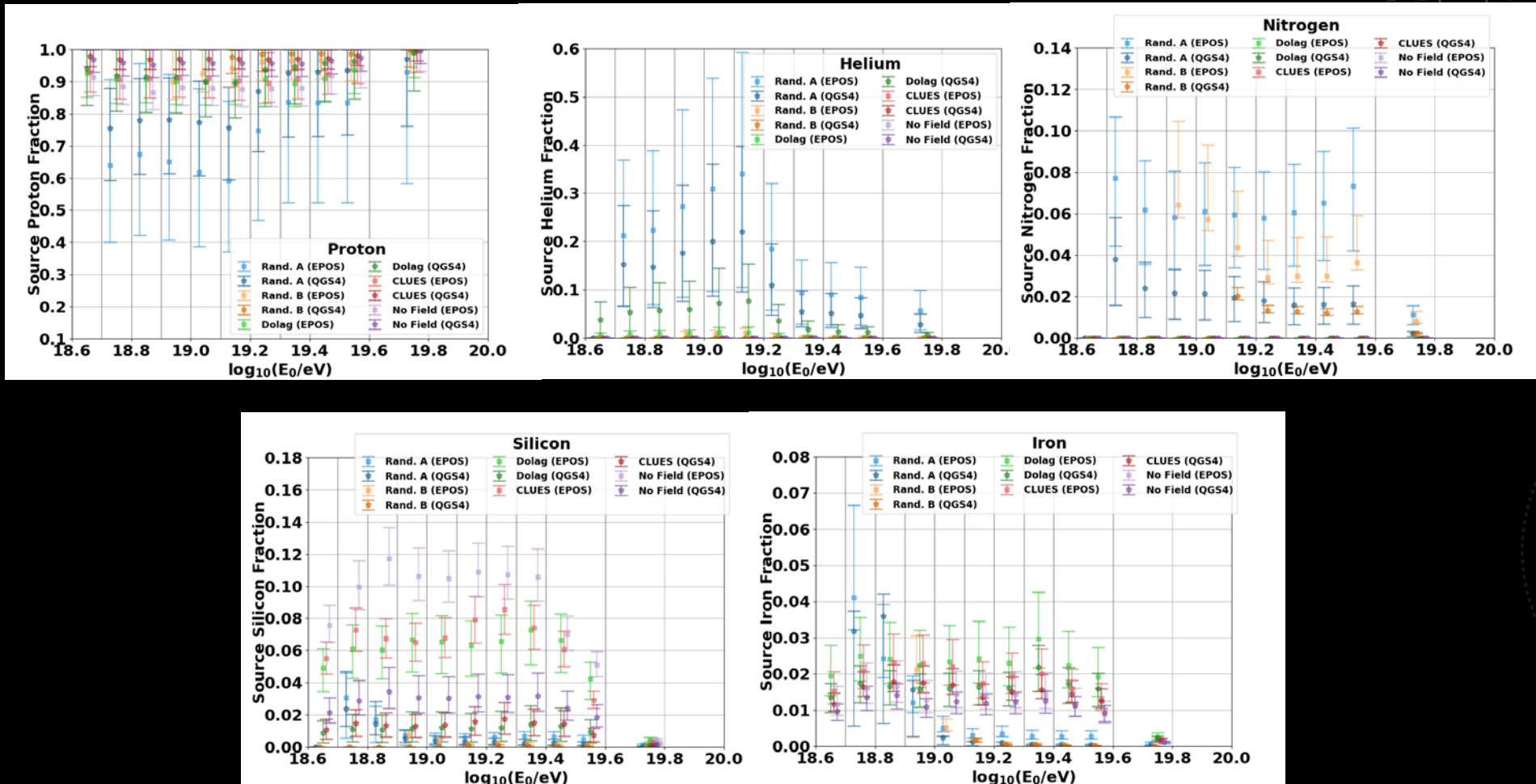
Observed Nuclei Fraction Versus Magnetic Field

SECONDARY RATIOS



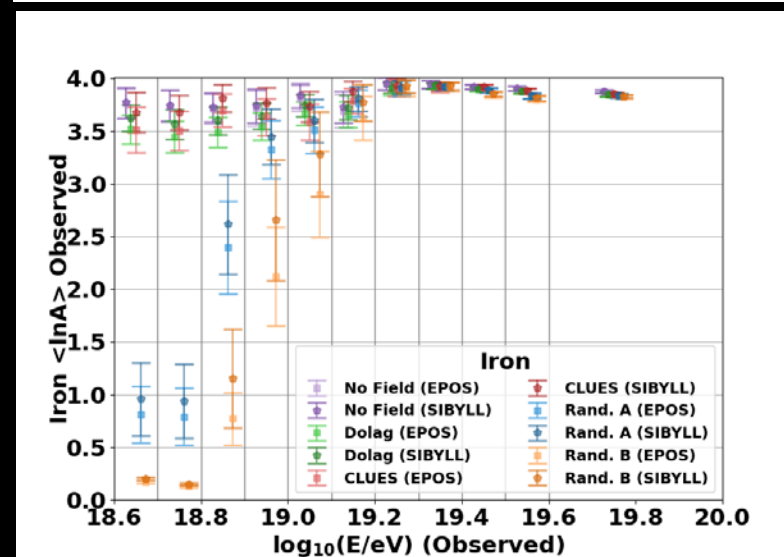
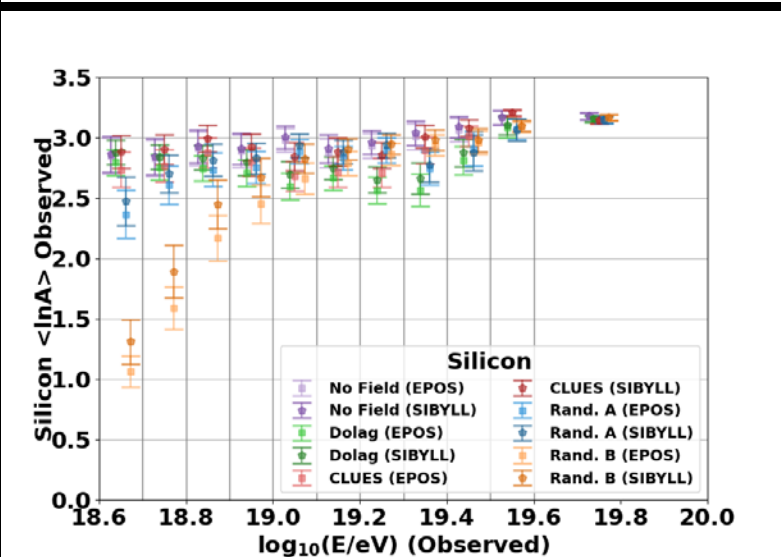
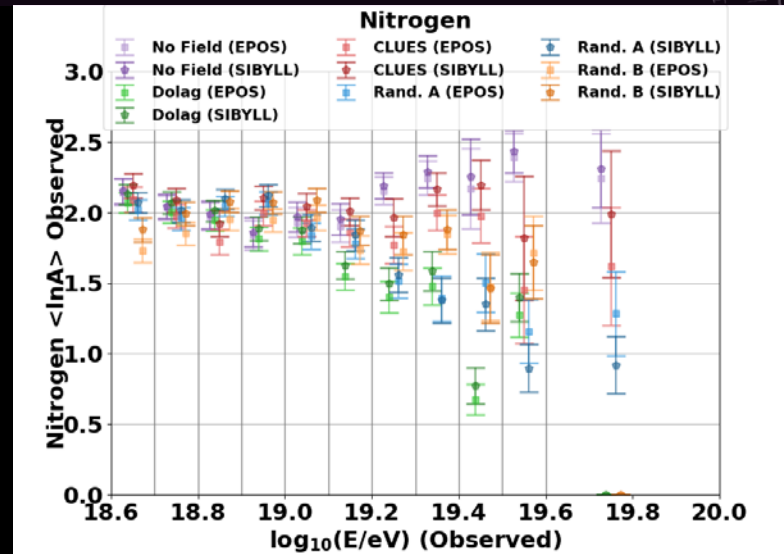
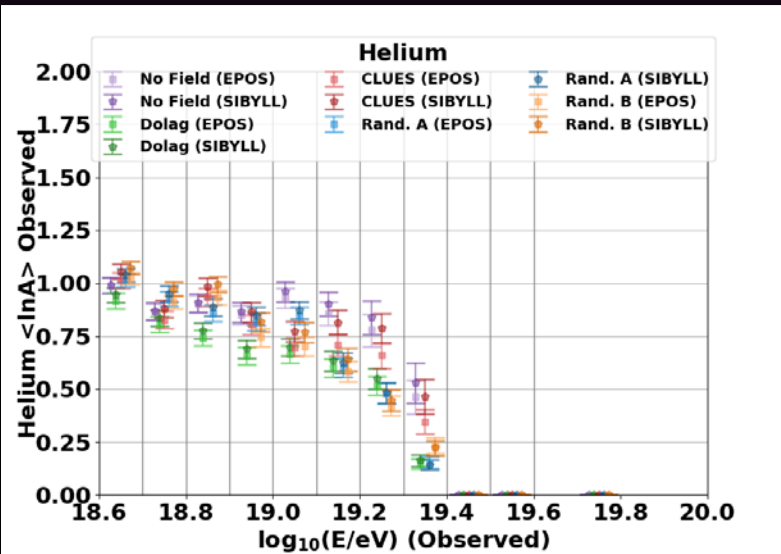
- Emitted energy binned ratios of observed secondaries to emitted nuclei.
- Total ratios used to convert constant observed fractions to emitted fraction.

FRACTIONS EMITTED

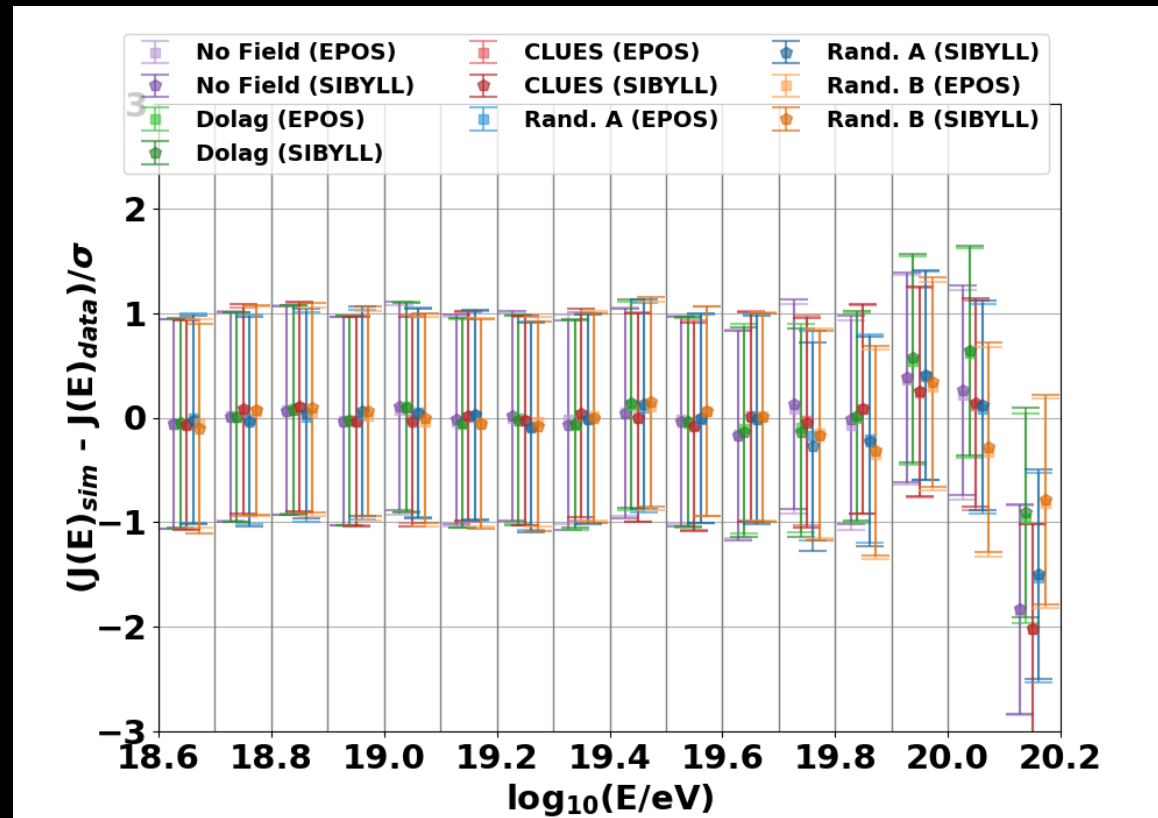


Emitted fractions in E_0 ins for observed constant fraction

OBSERVED $\langle \ln A \rangle$



ENERGY SPECTRUM FITS



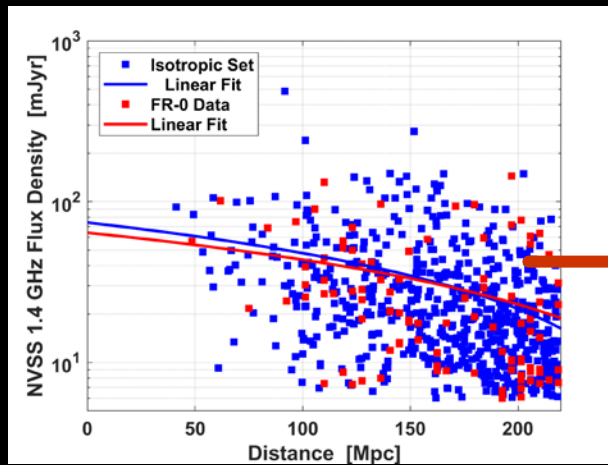
Energy Spectra Residuals for all models

EFFECT OF EXTENDING TO $z = 0.5$

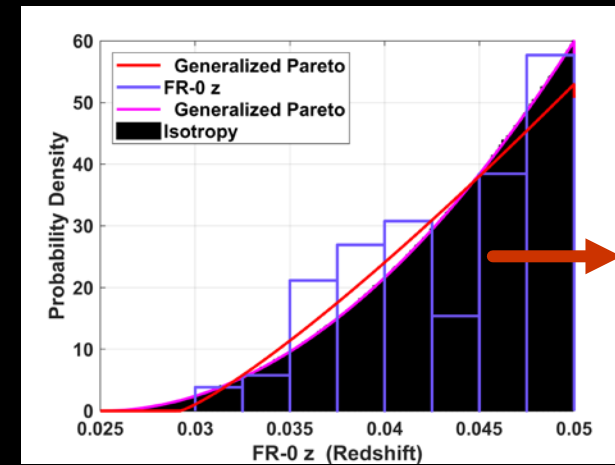
- 1 nG 234 kpc MAGNETIC FIELD

Extrapolating to FR0 sources $z = 0.05$ to 0.5 :

- Proton ratio (detected)/(emitted nuclei) is $\sim 1/24^{\text{th}}$ that of $z = 0$ to 0.05 .
 - Neutrinos (detected)/(emitted nuclei) is $\sim 1/68^{\text{th}}$.
- Iron ratio is $\sim 1/51^{\text{th}}$.
 - Neutrinos is $\sim 1/26^{\text{th}}$.
- **Results: small correction with significant computing penalty so we extended to $z = 0.2$**



1900



0.5

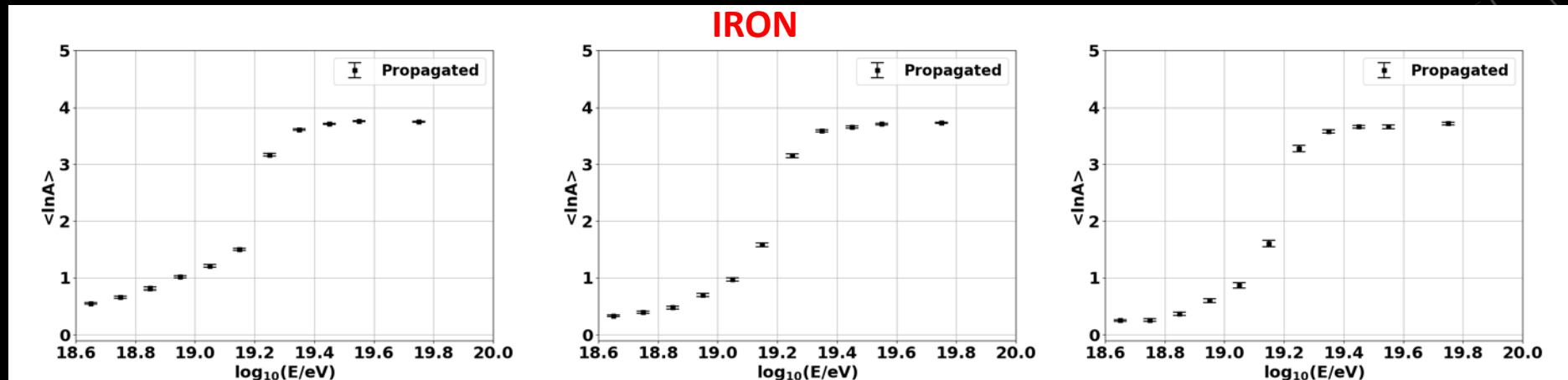
Local source evolution modeled by preserving correlation between radio output and redshift distance (Kendall's correlation coeff.: -0.28, p-Value: $4.6e-5$)[1].

Simulated FR-0 redshift distribution from Pareto fit to catalog data[1]. Isotropy probability of $\sim 16\%$.

EFFECT OF EXTENDING MAXIMUM Z

- IRON: 1 nG 234 kpc MAGNETIC FIELD

- Updated CRPropa 3
- Extrapolating to FRO sources $z = 0.05$ up to 0.5 (simulate 0 to 0.5)

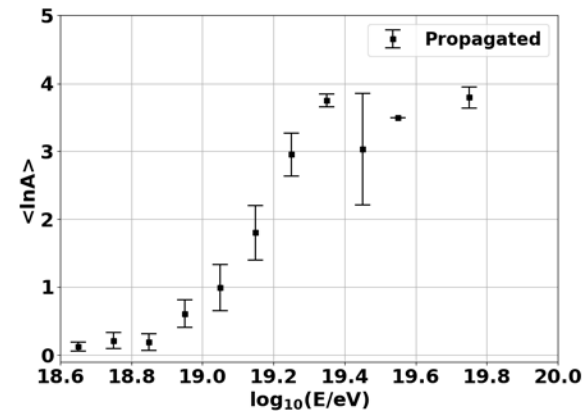


Up to $z = 0.05$

Up to $z = 0.1$

Up to $z = 0.2$

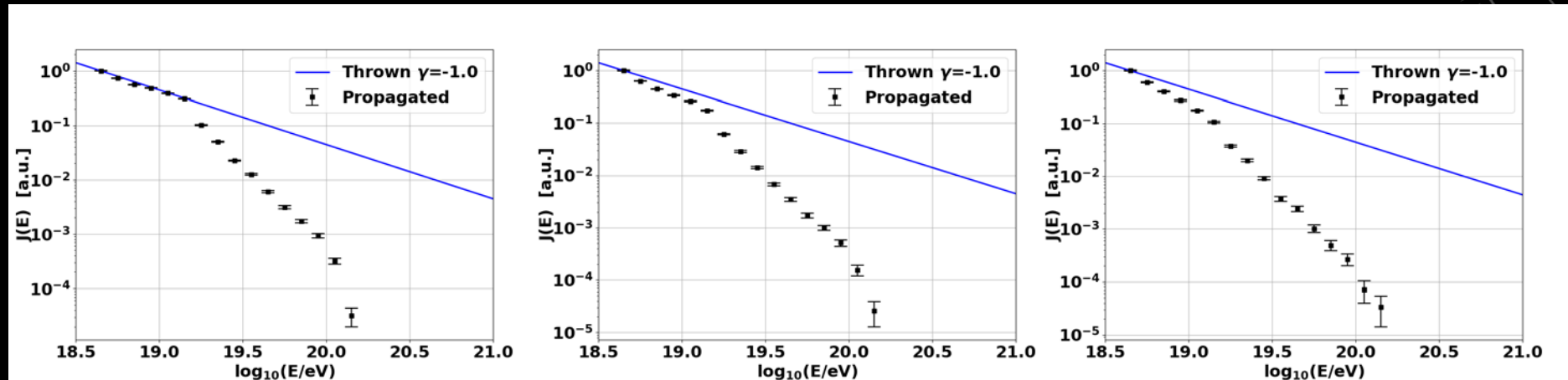
- Iron propagation does not change significantly past $z = 0.1$
- Up to $z = 0.5$ has too high computation cost.



EFFECT OF EXTENDING MAXIMUM Z

- IRON: 1 nG 234 kpc MAGNETIC FIELD

- Updated CRPropa 3
- Extrapolating to FRO sources $z = 0.05$ up to 0.5 (simulate 0 to 0.5)



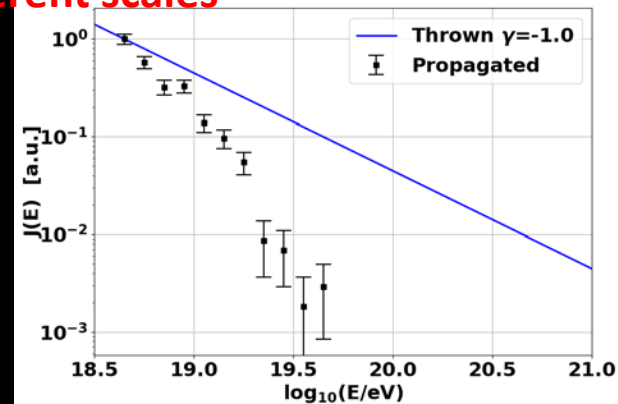
Up to $z = 0.05$

Up to $z = 0.1$

Up to $z = 0.2$

Different scales

- Iron propagation does not change significantly past $z = 0.1$
- Up to $z = 0.5$ has too high computation cost.

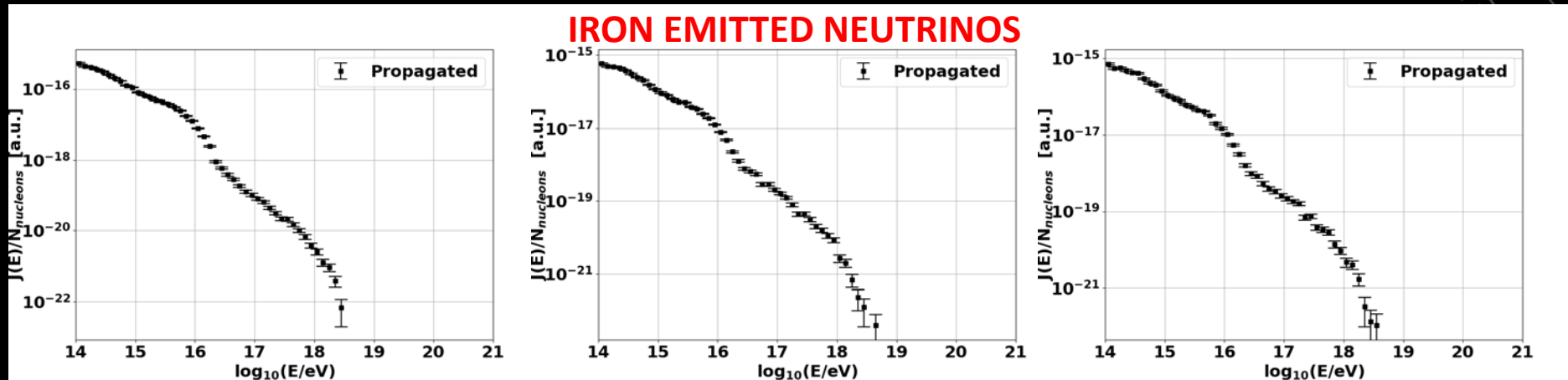


Up to $z = 0.5$
(smaller stats)

EFFECT OF EXTENDING MAXIMUM Z

- IRON EMITTED NEUTRINOS: 1 nG 234 kpc MAGNETIC FIELD

- Updated CRPropa 3
- Extrapolating to FRO sources $z = 0.05$ up to 0.5 (simulate 0 to 0.5)



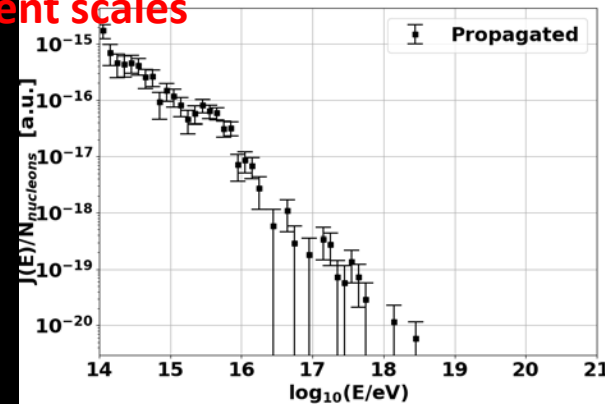
Up to $z = 0.05$

Up to $z = 0.1$

Up to $z = 0.2$

- Iron propagation does not change significantly past $z = 0.1$
- Up to $z = 0.5$ has too high computation cost.

Different scales

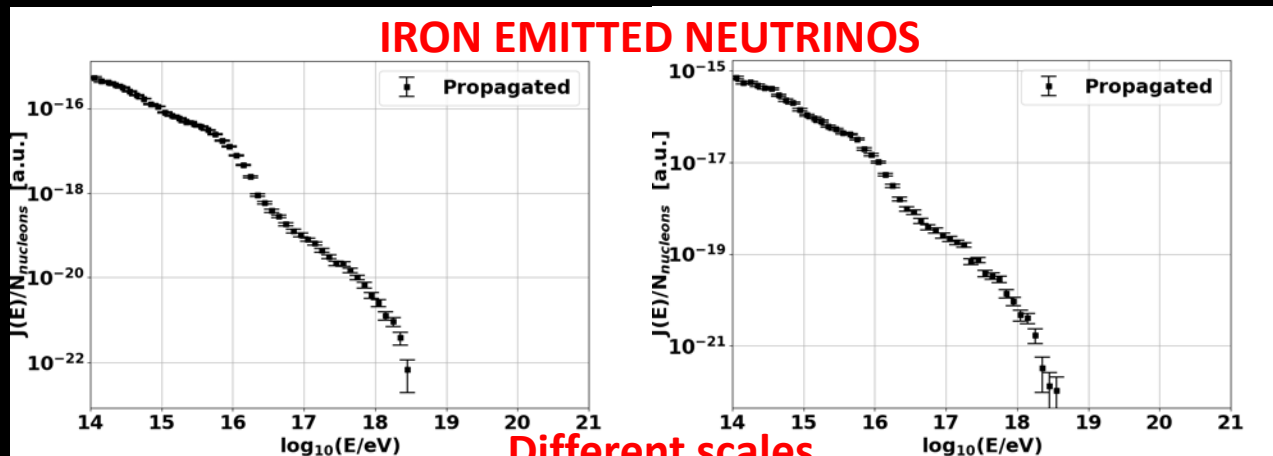


Up to $z = 0.5$
(smaller stats)

EFFECT OF EXTENDING MAXIMUM Z

- IRON EMITTED NEUTRINOS: 1 nG 234 kpc MAGNETIC FIELD

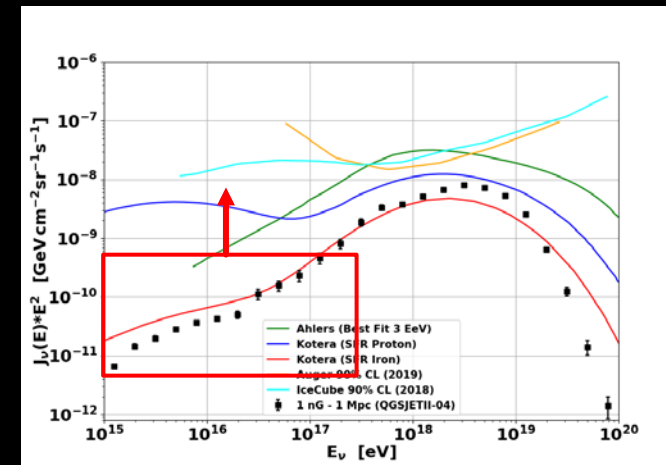
- Updated CRPropa 3
- Extrapolating to FRO sources $z = 0.05$ up to 0.5 (simulate 0 to 0.5)



Up to $z = 0.05$

Up to $z = 0.2$

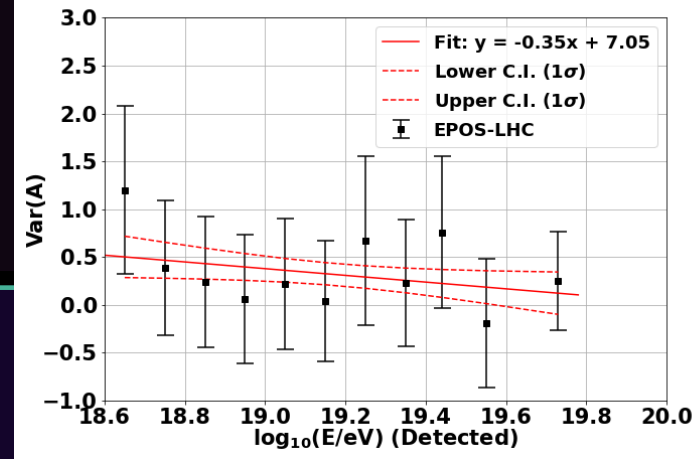
- More neutrinos.
 - Seems to affect lower energy more.



ADDING $\text{Var}(\ln A)$

- **EPOS-LHC $\text{Var}(\ln A)$**

- **Negative variances not calculable.**
- **Slope -0.29 ± 0.30**
 - **Not significant with uncertainties in A transform.**
 - **Transforming A to X_{\max} transfers uncertainty to simulation.**



- **Adding more rigid constraint than $\text{Var}(\ln A)$ χ^2 :**

- **Constrain simulation variance slope $\pm 1\sigma$.**

- χ^2 : 2.67 to 7.45
- Gamma γ : 2.67 to 3.14
- Rigidity cutoff: 37×10^{18} to 21×10^{18}
- Trajectory cutoff: 424 Mpc to 225 Mpc
- Observed nuclei fractions:

- Proton: 34% to 52%
- Helium: 27% to 0%
- H+He: 61% to 52%
- Nitrogen: 25% to 34%
- Silicon: 6% to 8.3%
- Iron: 7% to 5.4%

$z < 0.05$

1 nG 234 kpc magnetic field

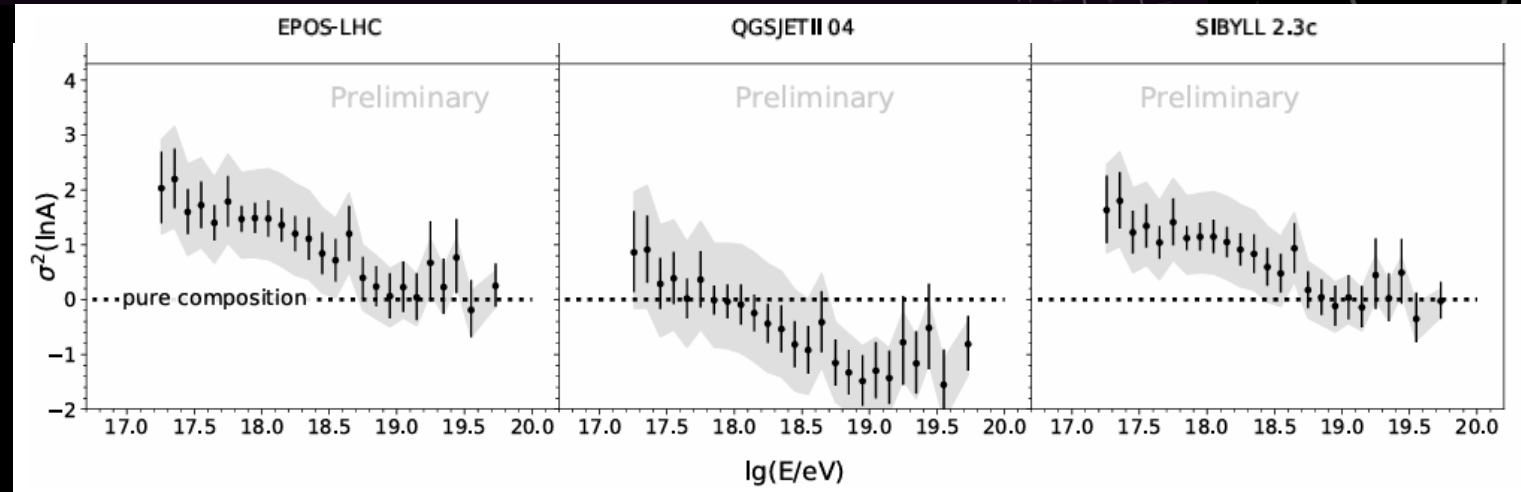
The background features several faint, light-colored technical diagrams. On the right side, there is a large circular diagram with concentric circles and radial lines, resembling a scale or a gauge, with numerical markings from 80 to 210. Below it is another circular diagram with dashed lines and arrows. On the left side, there are partial circular diagrams with arrows. A solid dark purple horizontal bar is centered across the middle of the image, containing the text 'EVOLVING FRACTION ADDITIONAL' in white, bold, uppercase letters.

EVOLVING FRACTION ADDITIONAL

VARIANCE RESULTS

- Var(lnA) for log₁₀(E) from 18.6 to 19.0**

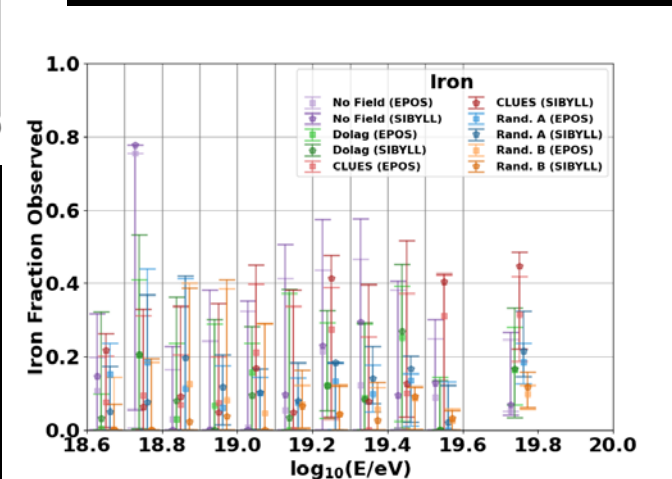
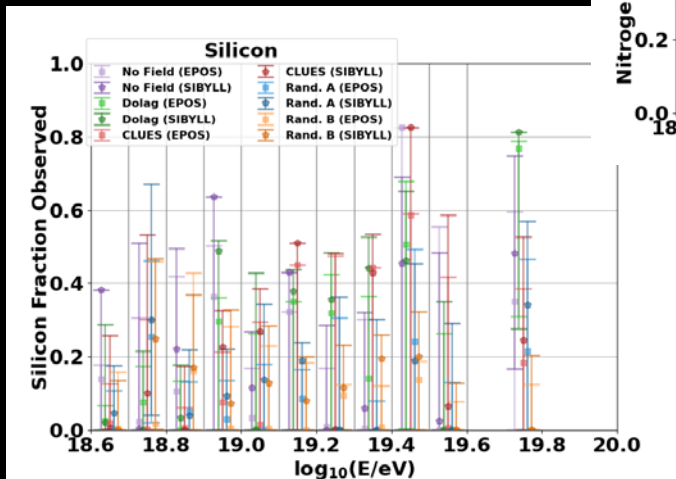
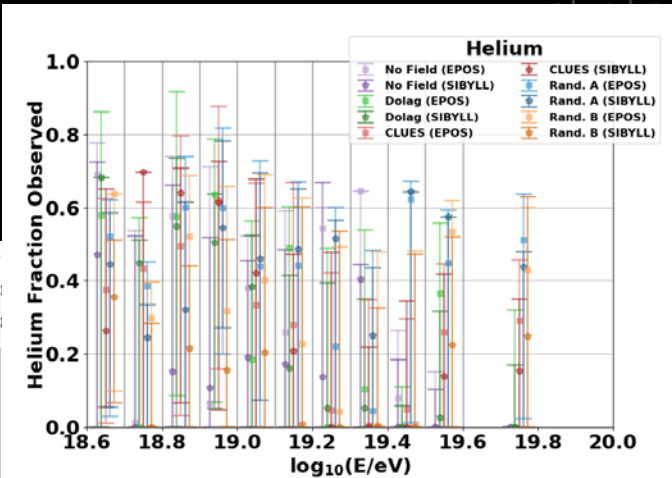
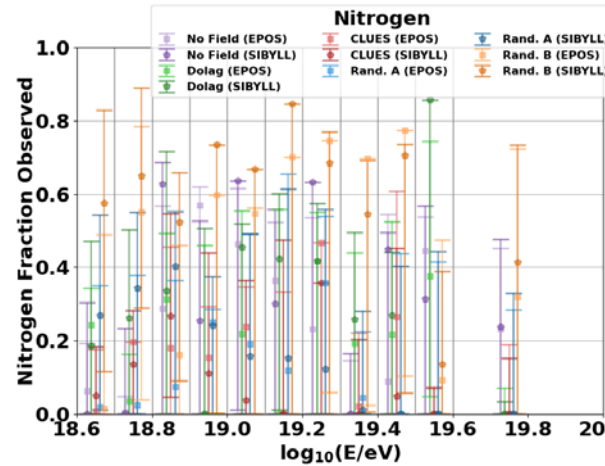
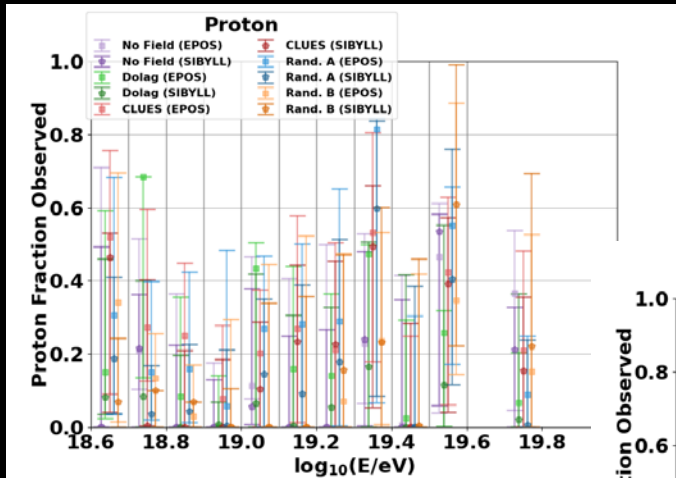
- No field-Sibyll: 2.31 ± 0.07
- No field-EPOS: 1.97 ± 0.10
- Dolag-Sibyll: 1.32 ± 0.04
- Dolag-EPOS: 1.64 ± 0.04
- CLUES-Sibyll: 1.44 ± 0.06
- CLUES-EPOS: 1.49 ± 0.05
- 1ng1mpc-Sibyll: 1.44 ± 0.04
- 1ng1mpc-EPOS: 1.25 ± 0.07
- 1ng3mpc-Sibyll: 1.11 ± 0.02
- 1ng3mpc-EPOS: 0.89 ± 0.03



**Data for log₁₀(E) from 18.5 to 19.0:
 1.64 ± 0.92**

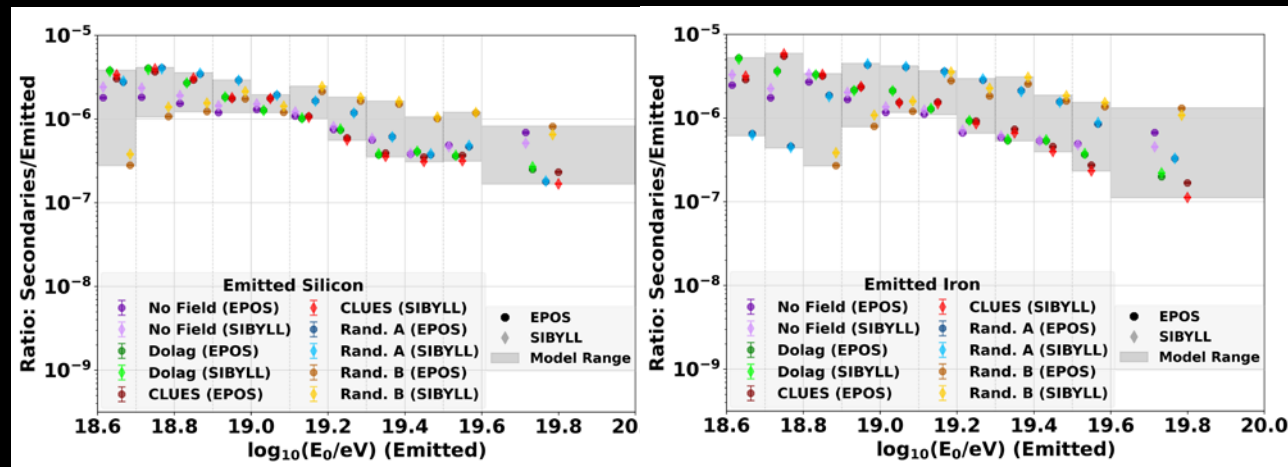
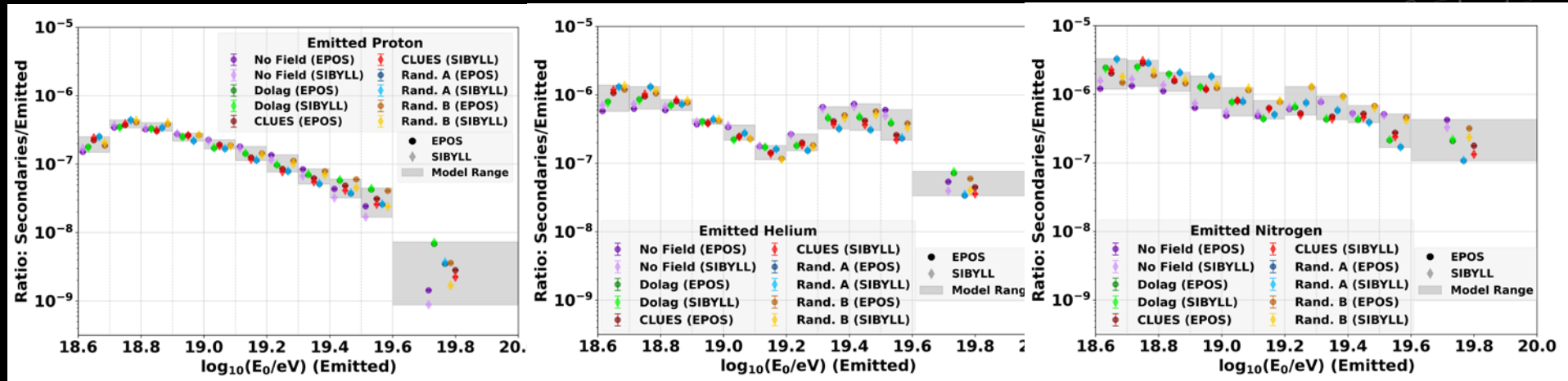
**Does not include muon uncertainty
Yushkov, A. 2020, PoS, ICRC2019, 482**

EVOLVING NUCLEI FRACTIONS (OBSERVED)



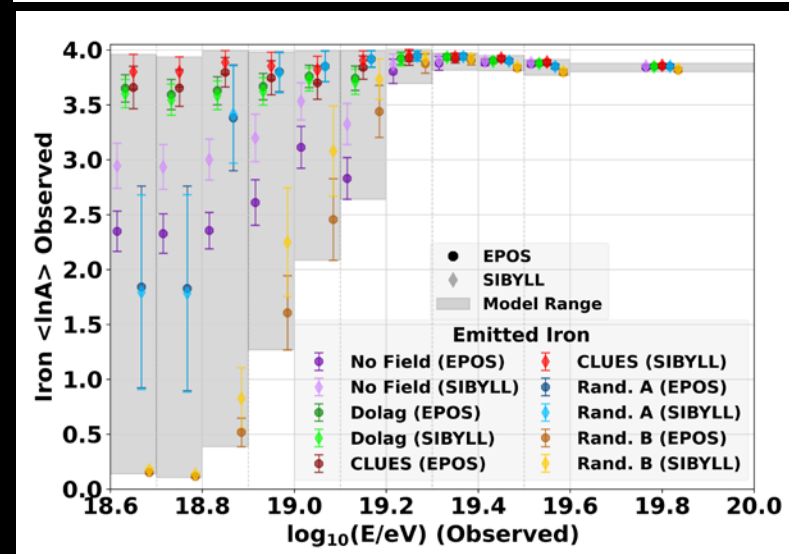
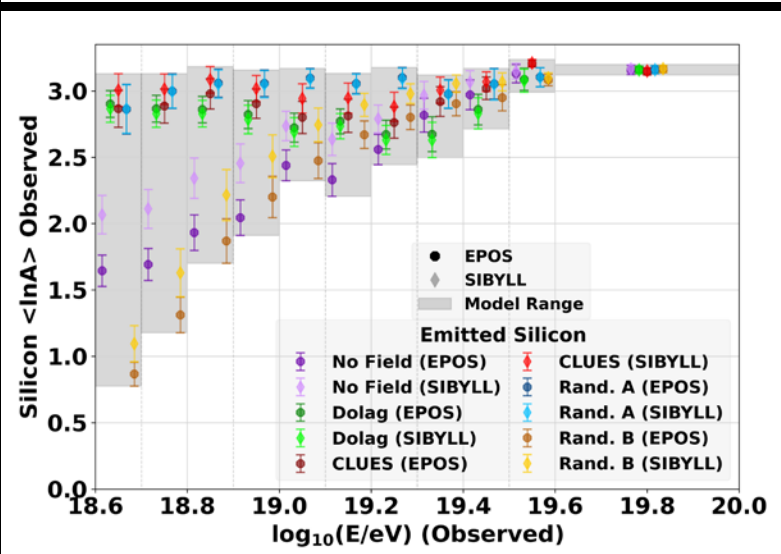
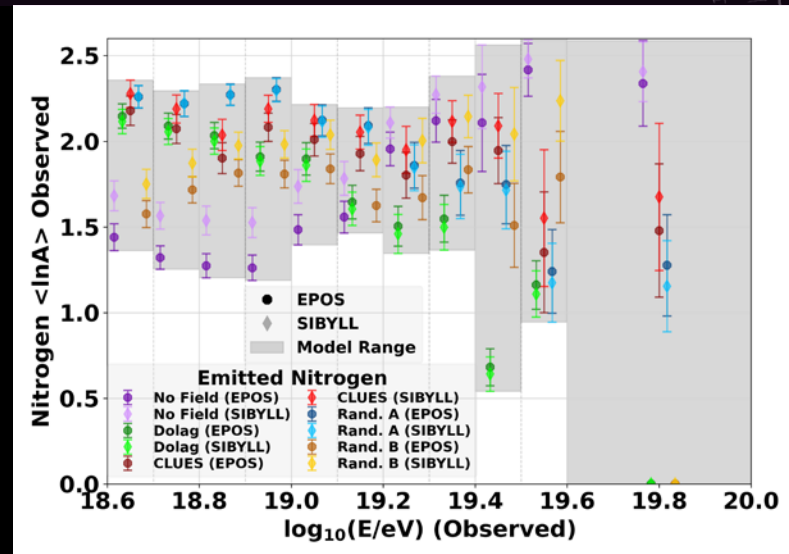
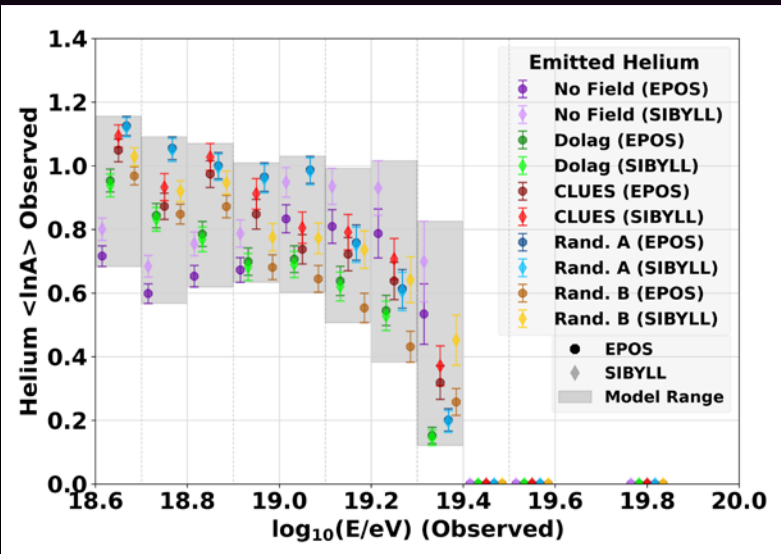
Observed Nuclei Fraction Versus Magnetic Field

SECONDARY RATIOS



Used to convert observed fractions to emitted fractions

OBSERVED $\langle \ln A \rangle$



FIT RESULT TABLES

Table 5. Evolving Fraction Energy Spectrum Parameters

Field	Model	$\Sigma\chi^2/\text{bin}$	γ	$\log_{10}(R_{\text{cut}}/V)$	$D_{\text{cut}}/\text{Mpc}$	n
No Field	SIBYLL	0.370	$2.10^{+0.47}_{-0.14}$	$19.19^{+0.84}_{-0.20}$	844^{+0}_{-1}	$1.344^{+0.014}_{-0.005}$
	EPOS	0.326	$1.94^{+0.60}_{-0}$	$19.22^{+0.75}_{-0.01}$	844^{+0}_{-1}	$1.343^{+0.006}_{-0.005}$
Dolag	SIBYLL	0.469	$2.28^{+0.14}_{-0.84}$	$19.89^{+0.31}_{-0.98}$	907^{+450}_{-50}	$1.328^{+0.023}_{-0.000}$
	EPOS	0.446	$2.31^{+0.12}_{-0.20}$	$19.89^{+0.40}_{-0.38}$	889^{+146}_{-39}	$1.342^{+0.006}_{-0.011}$
CLUES	SIBYLL	0.307	$2.65^{+0.00}_{-0.29}$	$19.58^{+0.27}_{-0.25}$	841^{+1}_{-0}	$1.342^{+0.013}_{-0.007}$
	EPOS	0.295	$2.52^{+0.09}_{-0.22}$	$19.58^{+0.51}_{-0.20}$	842^{+0}_{-1}	$1.342^{+0.006}_{-0.004}$
Rand.A	SIBYLL	0.344	$2.64^{+0.20}_{-0.25}$	$19.95^{+0.50}_{-0.56}$	855^{+93}_{-7}	$1.343^{+0.008}_{-0.005}$
	EPOS	0.341	$2.65^{+0.05}_{-0.30}$	$19.89^{+0.94}_{-0.32}$	844^{+113}_{-0}	$1.342^{+0.006}_{-0.006}$
Rand.B	SIBYLL	0.236	$2.35^{+0.34}_{-0.30}$	$19.40^{+1.64}_{-0.32}$	843^{+171}_{-0}	$1.346^{+0.009}_{-0.006}$
	EPOS	0.237	$2.21^{+0.34}_{-0.45}$	$19.51^{+1.20}_{-0.38}$	843^{+174}_{-0}	$1.342^{+0.004}_{-0.007}$

Notes. The FR0 evolving fraction combined fit results total sum chi-square per bin, spectral index γ , exponential rigidity cutoff ($\log_{10}(R_{\text{cut}}/V)$), trajectory cutoff (D_{cut}), and spectrum normalization for all 10 configurations. The two EAS are EPOS-LHC (EPOS) and Sibyll2.3c (SIBYLL).

FIT RESULT TABLES

Table 6. Evolving Fraction Bootstrap Energy Spectrum Parameters

Field	Model	$\Sigma\chi^2/\text{bin}$	γ	$\log_{10}(R_{\text{cut}}/V)$	$D_{\text{cut}}/\text{Mpc}$	n
No Field	SIBYLL	0.370	$2.44^{+0.23}_{-0.23}$	$19.34^{+0.25}_{-0.25}$	843^{+0}_{-0}	$1.345^{+0.006}_{-0.006}$
	EPOS	0.326	$2.47^{+0.12}_{-0.12}$	$19.40^{+0.10}_{-0.10}$	843^{+0}_{-0}	$1.340^{+0.004}_{-0.004}$
Dolag	SIBYLL	0.469	$2.26^{+0.28}_{-0.28}$	$19.23^{+0.25}_{-0.25}$	867^{+193}_{-193}	$1.335^{+0.004}_{-0.004}$
	EPOS	0.446	$2.26^{+0.19}_{-0.19}$	$19.74^{+0.18}_{-0.18}$	890^{+107}_{-107}	$1.341^{+0.003}_{-0.003}$
CLUES	SIBYLL	0.307	$2.40^{+0.07}_{-0.07}$	$19.71^{+0.12}_{-0.12}$	842^{+0}_{-0}	$1.347^{+0.013}_{-0.007}$
	EPOS	0.295	$2.34^{+0.06}_{-0.06}$	$19.68^{+0.10}_{-0.10}$	842^{+0}_{-0}	$1.341^{+0.005}_{-0.005}$
Rand.A	SIBYLL	0.344	$2.37^{+0.05}_{-0.05}$	$19.83^{+0.11}_{-0.11}$	853^{+35}_{-35}	$1.342^{+0.003}_{-0.003}$
	EPOS	0.341	$2.33^{+0.05}_{-0.05}$	$19.68^{+0.08}_{-0.08}$	851^{+30}_{-30}	$1.342^{+0.003}_{-0.003}$
Rand.B	SIBYLL	0.236	$2.41^{+0.10}_{-0.10}$	$19.74^{+0.41}_{-0.41}$	850^{+43}_{-43}	$1.348^{+0.004}_{-0.004}$
	EPOS	0.237	$2.31^{+0.11}_{-0.11}$	$19.59^{+0.20}_{-0.20}$	853^{+49}_{-49}	$1.345^{+0.004}_{-0.004}$

Notes. The FR0 evolving fraction combined fit bootstrap distribution most probable spectral index γ , exponential rigidity cutoff ($\log_{10}(R_{\text{cut}}/V)$), trajectory cutoff (D_{cut}), and spectrum normalization for all 10 configurations.